International Journal of Hydrogen Energy 198 (2026) 152325

Contents lists available at ScienceDirect

International Journal of Hydrogen Energy

journal homepage: www.elsevier.com/locate/he

Techno-economic analysis of a renewable hydrogen refuelling station network: The case study of Spain

Beatriz Garcia Minguez [a], Pol Cardona [a,*], Luis Valiño [c], Carlos Ocampo-Martinez [b], Lukas Siemon [d], Maria Serra [a]

[a] Institut de Robòtica i Informàtica Industrial, CSIC-UPC, Llorens i Artigas 4-6, 08028 Barcelona, Spain
[b] Automatic Control Department (ESAII), Universitat Politècnica de Catalunya - BarcelonaTECH, Av. Diagonal, 647, 08028 Barcelona, Spain
[c] Instituto de Carboquímica (Consejo Superior de Investigaciones Científicas), C/ de Miguel Luesma Castán, 4, 50018 Zaragoza, Spain
[d] Chair of Sustainable Manufacturing and Life Cycle Engineering, Institute of Machine Tools and Production Technology (IWF), Technische Universität Braunschweig, Langer Kamp 19B, 38106 Braunschweig, Germany

ARTICLE INFO

Keywords:
Hydrogen refuelling station
On-site hydrogen production
Fuel cell electric vehicles
HOMER

ABSTRACT

Hydrogen-powered Fuel Cell Electric Vehicles (FCEVs) offer a promising pathway to reduce emissions of the transport sector, particularly when fuelled by renewable hydrogen produced through water electrolysis using Renewable Energy Sources (RESs). However, adoption is constrained by the limited refuelling infrastructure and the current higher readiness and competitiveness of battery electric and hybrid alternative technologies for the traction system. In response, the Spanish government aims to install 100 to 150 HRSs nationwide by 2030 amongst other objectives for the hydrogen infrastructure. This paper introduces a Spain-wide, RES-clustered design and assessment of the renewable HRS network that jointly (i) estimates light- and heavy-duty FCEV demand anchored to national targets, grounded forecasts and empirical refuelling patterns (ii) optimally decides per each RES zone the distribution and capacity using two station scales (daily hydrogen throughput capacity) and (iii) analyzes the on-grid and off-grid HRS design requirements and techno-economic results of their deployment. The clustering of the Spanish territory is performed to discretize the simulation and analysis geographically, and the clusters are decided based on RES potential. The main core of the techno-economic modelling and simulation is carried out via a coordinated HDRSAM–HOMER workflow that improves on common approaches presented in the literature, where only one of these tools is considered. The results reveal that off-grid stations have a Levelized Cost of Hydrogen (LCOH) ranging from 14.79 $/kg to 24.13 $/kg, with larger stations benefiting from modest economies of scale. By contrast, on-grid HRSs present lower LCOH (9.56–16.71 $/kg) and a significantly lower energy surplus than that in off-grid topologies. Consequently, grid connectivity proves advantageous in regards to energy utilization and cost. These findings provide a robust foundation for scaling a renewable HRS network rollout in Spain, underscoring the role of on-grid solutions in accelerating FCEV adoption and enhancing sustainable mobility while keeping RES input necessary to optimize costs and reduce emissions.

1. Introduction

Renewable hydrogen, produced using Renewable Energy Sources (RES), has emerged as an enabler to decarbonize the transportation sector, driven by the growing urgency to address climate change. Hydrogen is an effective energy carrier due to its high energy density, producing no direct emissions [1]. This shift is significant in Spain, where transportation accounts for the highest contribution, 32.5% as of 2023, in greenhouse gas emissions among all contributing sectors [2,3]. Furthermore, Spain ranks second and fourth out of the EU-27 member states for installed wind and PV capacity, respectively [4,5]. These facts provide a favourable environment for producing green hydrogen using water electrolysis. A key barrier to the widespread implementation of hydrogen-based transportation is the persistent chicken-and-egg dilemma between establishing a robust hydrogen supply network and achieving widespread adoption of Fuel Cell Electric Vehicles (FCEVs) [6]. To overcome this problem, the Spanish government has proposed a roadmap to deploy 150 Hydrogen Refuelling Stations (HRSs) by 2030 [7]. Establishing an HRS network is challenging and highly complex for various reasons. Renewable hydrogen production, primarily through water electrolysis, remains expensive due to the high

* Corresponding author.
E-mail address: pol.cardona@upc.edu (P. Cardona).

https://doi.org/10.1016/j.ijhydene.2025.152325
Received 4 July 2025; Received in revised form 20 September 2025; Accepted 29 October 2025
Available online 26 November 2025
0360-3199/© 2025 The Authors. Published by Elsevier Ltd on behalf of Hydrogen Energy Publications LLC. This is an open access article under the CC BY-NC-ND license (http://creativecommons.org/licenses/by-nc-nd/4.0/).

List of Abbreviations

AC	Autonomous Community
AEM	Anion Exchange Membrane (electrolyzer technology)
CCUS	Carbon Capture, Utilization and Storage
CO_2	Carbon Dioxide
CRF	Capital Recovery Factor
FCEV	Fuel Cell Electric Vehicle
FCLM	Fuel Capture Location Model
GHG	Greenhouse Gas
GHI	Global Horizontal Irradiance
HD-FCEV	Heavy-Duty Fuel Cell Electric Vehicle
HDRSAM	Heavy-Duty Vehicle Refuelling Cost Model
HDRSAM	Hydrogen Demand and Resource Scenario Analysis Model
HDSAM	Hydrogen Delivery Scenario Analysis Model
HOMER	Hybrid Optimization of Multiple Energy Resources
HRS	Hydrogen Refuelling Station
HRSAM	Hydrogen Refuelling Station Analysis Model
ICEV	Internal Combustion Engine Vehicle
IEA	International Energy Agency
LCOH	Levelized Cost of Hydrogen
LD-FCEV	Light-Duty Fuel Cell Electric Vehicle
NLP	Non-Linear Programming
NPC	Net Present Cost
O&M	Operation and Maintenance
PEM	Polymer Electrolyte Membrane (electrolyzer technology)
PV	Photovoltaic
RES	Renewable Energy Sources
SMR	Steam Methane Reforming
TEA	Techno-economic analysis
WT	Wind Turbine

Nomenclature

CRF	Capital Recovery Factor
NPC	Net Present Cost (USD)
c_L	Capacity of a large HRS (kg/day)
c_S	Capacity of a small HRS (kg/day)
C_{ann}	Annualized cost of the system (USD/year)
C_{inv}	Investment costs (USD)
$C_{O\&M}$	Operating and maintenance costs (USD)
C_{rep}	Replacement costs (USD)
C_S	Salvage value (USD)
d_i	Hydrogen demand in ACi (kg/day)
i	Nominal discount rate (%)
J	Cost function in the optimization problem
M_{H_2}	Annual hydrogen production (kg/year)
n	Total number of Autonomous Communities
r_{real}	Real discount rate (%)
R_{Grid}	Revenue from selling power to the grid (USD/year)
S_i	Required minimum HRSs in ACi
$x_{L,i}$	Number of large HRSs in ACi
$x_{S,i}$	Number of small HRSs in ACi

costs of renewable electricity and electrolysis equipment compared to other hydrogen production methods, which involve fossil fuels [8]. Besides the production of hydrogen, the interdependencies and challenges of compression, storage and transportation of hydrogen require that the widespread use of hydrogen is assessed systematically, addressing temporal and spatial characteristics of hydrogen demand and supply.

1.1. Trends in the hydrogen economy

In 2022, 95 Mt of hydrogen were produced worldwide, yet only 0.75% was produced using green hydrogen production methods, mainly from fossil fuels with Carbon Capture, Utilization and Storage (CCUS) or generated using electricity via electrolysis. These two methods accounted for 0.6% and 0.15% of the global hydrogen production, respectively. Despite hydrogen's growing prominence, its use remains predominantly concentrated within traditional sectors such as steel manufacturing and refining, and in chemical industries producing ammonia, methanol, and other derivatives. Conversely, emerging sectors such as transportation and power generation consumed a negligible share (0.1%) of the total hydrogen produced [9]. It is important to highlight that the dominant role of hydrogen in hard-to-abate sectors, especially steel and refining, is expected to persist or even strengthen in the future, potentially taking precedence over new applications like transportation. This competition for renewable hydrogen supplies could significantly impact the FCEVs adoption trajectory and the associated infrastructure requirements. Nevertheless, even under the expected scenario where transportation does not emerge as a leading hydrogen consumer, the current state of hydrogen infrastructure remains infant. Therefore, any incremental growth in FCEV adoption will necessitate substantial infrastructure development relative to the existing baseline.

In this context, it is relevant to understand the current state of the FCEV market. By the end of 2023, the global fleet of FCEVs had reached 80,000 units, with Korea retaining its position as the primary market for light-duty (LD) FCEVs and China for heavy-duty (HD) FCEVs. Although the number of LD-FCEVs surpasses the number of 8000 HD-FCEVs, the latter accounts for a significantly larger share of hydrogen consumption. In LD-FCEVs, hydrogen gas is usually stored in high-pressure tanks at 700 bar, whereas in HD-FCEVs, such as buses and trucks, hydrogen is usually stored at 350 bar, although 700 bar models are also currently on the market [10]. The latter are cheaper and more energy-efficient than 700-bar tanks. However, LD-FCEVs have limited storage space, requiring the use of higher-pressure tanks due to volume constraints [11]. Refuelling hydrogen tanks of LD-FCEVs takes 3 to 5 min for typical tank capacities of 5 to 6 kg of hydrogen. For HD-FCEVs, the typical time is approximately 10 min for capacities of around 30 kg of hydrogen [10,12–15].

While China only accounts for 20% of the global fleet of FCEVs, they consume more than half of the global hydrogen demand for road transport [9]. In Europe, as of July 2024, the total number of FCEVs was 5570, with Germany leading at 2273 units [16]. Regarding the hydrogen refuelling infrastructure, as of June 2023, there were almost 1100 HRSs in operation globally. Specifically, China leads with 350 stations, followed by Europe with over 250 stations [9,17]. Similarly to the distribution of FCEVs, Germany has the highest number of HRSs with 117 units [17].

According to the Hydrogen Council [18], the global number of FCEVs is estimated to reach 13 million units by 2030, including 1 M commercial vehicles for freight transportation. In Europe, the estimate is approximately 4,2 M FCEVs, including 45,000 commercial vehicles. The forecasts for HRS estimate approximately 3700 units for Europe and more than 10,000 worldwide [18]. In 2015, the International Energy Agency (IEA) estimated a rollout scenario of 30,000 FCEVs and 680 HRSs across the USA, Japan and Europe by 2020 [19]. This goal was surpassed; by 2023, 80,000 FCEVs and 1100 HRSs were recorded worldwide. For 2030, the forecast included 8 M FCEVs and 16,000 HRSs; for 2050, 150 M FCEVs and 57,000 HRSs respectively [19]. Moreover, the Clean Hydrogen Partnership [20] estimated 1500 HRSs with a capacity of 1000 kg per day, to be deployed by 2025 in Europe.

Table 1
Summary of estimated and current HRSs and FCEVs.

Region	Current HRSs	Current FCEVs	Source	Year of Study	Year of Estimate	Estimated HRSs	Estimated FCEVs
Global	1,100	80,000	Hydrogen Council [18]	2020	2030	10,000	13 M
			IEA [1]	2015	2030	16,000	8 M
			IEA [1]	2015	2050	57,000	150 M
Europe	254	5,570	Hydrogen Council [18]	2020	2030	3,700	4.2 M
			Clean HydrogenPartnership [20]	2019	2025	1,500	–
			Clean HydrogenPartnership [20]	2019	2030	3,700	22% market share
			Iordache et al. [21]	2017	2030	3,000	14 M
Spain	3	29	MITECO [7]	2020	2030	150	7,700
			Clean HydrogenPartnership[20]	2019	2025	15	–
			Iordache et al. [21]	2017	2030	564	1.2 M
			Funez Guerra et al. [22]	2016	2030	68	475,620

Comparing the estimates from 2019 for 2030 to the current development in 2024 [17], in Europe only 17% of the proposed forecast for HRS has been achieved. The 2025 forecast for FCEVs stated by the Clean Hydrogen Partnership [20] estimated about 800,000 units. By 2030, the FCEV market penetration rate is estimated at 22%, including 3700 HRSs [18]. Table 1 summarizes the forecasts for HRSs and FCEVs for Spain, Europe and worldwide.

In 2023, only 29 FCEVs were recorded in Spain, consisting of 23 passenger vehicles and six buses [16]. This fact places Spain in the lowest position at the European level. Currently, three HRSs are open to the public [23,24] located in Huesca, Puertollano and Albacete, offering hydrogen at 700 bar for LD-FCEV. Moreover, there are 44 HRS projects comprising 19 private and 25 public projects [25]. In 2020, the Spanish government introduced a hydrogen roadmap with the goal of installing by 2030 at least 4 GW of capacity for the generation of hydrogen based on electrolysis. The plan envisions a fleet of 150 to 200 fuel cell buses and 5000 to 7500 light and heavy-duty FCEV for freight transport. The roadmap also outlines the development of a network of 100 to 150 publicly accessible HRSs to support these vehicles. Additionally, the roadmap includes adopting hydrogen technologies in other sectors, such as railway transport. The government has allocated a total budget of 8900 Me to achieve the objectives outlined in the roadmap [7].

Spain's abundant RES potential and installed capacity enables the production of renewable hydrogen through water electrolysis. As of 2023, the energy mix in Spain consisted of 53% of RESs with 40.4 TWh of solar PV-generated energy, 61.1 TWh wind-generated energy and 24.2 TWh of hydroelectric energy [26]. Spain is the 7th country in the world with the highest installed photovoltaic capacity [27], accounting for 25,5 GW [28]. Extremadura and Castilla-La Mancha are the regions with the highest installed photovoltaic capacity in the country, with more than 6 GW. The southern regions have a higher PV potential (Andalucía, Extremadura and Castilla-La Mancha) than the northern regions (Galicia, Asturias and País Vasco). As of 2024, there are 1345 wind farms with more than 22,000 wind turbines installed in Spain, accumulating 29.8 GW of wind capacity [29]. The region with the highest wind energy production is Castilla *y* León with 6.5 GW installed capacity.

1.2. Methods for assessing HRS networks in literature

Establishing an HRS network is challenging and highly complex. Renewable hydrogen production, primarily through water electrolysis, remains expensive compared to fossil-derived hydrogen, and the limited refuelling infrastructure reinforces a chicken-and-egg dilemma between FCEV adoption and HRS deployment. Numerous studies have conducted Techno-Economic Analyses (TEAs) of HRSs to address these challenges. Studies conducting TEAs on HRSs can show patterns in the focus and perspective taken on both the technical and the economic aspects. On the technical side, the literature discusses grid connection and RES interaction, on- vs./off-site production and delivery, technology choices across storage and production stages, and sizing from aggregate capacity (daily delivery) down to detailed parameters such as delivery pressure, storage volumes and pre-cooling capacity. Concerning economic aspects, studies mainly focus on obtaining common indicators, such as the Net Present Cost (NPC) and the Levelized Cost of Hydrogen (LCOH), accompanied by an assessment and breakdown in terms of the technical aspects in question, which are normally tackled with a sensitivity analysis. A recurring gap in broader-scoped TEAs (at the network level) is the treatment of demand. While demand is often aggregated as a smooth hourly or daily profile, HRS demand is intrinsically event-triggered (the dispenser is either occupied or not). Initial and end-point conditions during short refuelling processes (3–15 min) matter, especially pressure, which drives compression strategy, cascaded storage sizing and cooling, with effects propagating upstream up to the production stage. Treating the station as a generic energy supply point would only hold for topologies dispensing directly from a compressor; common HRS designs rely on natural outflow from high-pressure storage to the vehicle tank, so the delivered mass depends on the mass–volume–pressure relation and the staging of pressures.

Most TEAs follow a common workflow, as seen in [31,32,35,41,42]. First, case-study locations are selected, and scope/site-specific RES data (solar irradiance, wind speeds) are imported. Second, hydrogen demand is specified, often as an hourly profile, a fixed number of daily refuelling events or a fleet mass-per-day target. Third, the technical specifications of the HRS layout and components are determined. These specifications encompass mainly performance and capacity parameters for electrolyzers, storage tanks, compressors, and other necessary equipment. Often, the capacities of the components are calculated using specific equations. Fourth, linear techno-economic parameters (capacity-to-cost conversion) are defined for each HRS component. Finally, an economic assessment estimates NPC and LCOH values normally accompanied by a sensitivity analysis mainly focused on RESs input, topology variations, component specifications, demand fluctuations or even factors such as electricity prices due to regionality, as is the case of [36]. Although the methodology taken is quite similar, reported LCOH values span a wide range due to differences in topology (on-/off-grid), energy supply and hydrogen production method; an overview of these values is presented in Table 2. The LCOH values presented in Table 2 should be considered as relative indicators since boundaries and financial assumptions may differ across studies. Additionally, the variability of component prices with technical characteristics, manufacturer and daily dispensing capacity may further complicate HRS cost calculations [43]. In aggregate, total capital costs reported for HRSs range approximately from 1 M$ to 7 M$, depending on station size, component selection and hydrogen capacity [13,30–32,44]. In addition to the common workflow, TEAs can be grouped regarding the scope, if they either study a unique location, a city, a region, or a nation. Depending on the scope, the aforementioned workflow may be slightly modified, although the pivotal steps are usually maintained. Regarding site-specific locations, they are either

Table 2
LCOH of different HRS studies.[a].

Reference	LCOH ($/kg)	Capacity (kg/day)	Hydrogen production	On/off-grid
[30]	8.38	100	On-site electrolysis	on-grid
[31]	6.34 - 8.97	125	Wind-powered electrolysis	off-grid
[32]	8.71	450	PV-powered electrolysis	on-grid
[33]	2.73 - 5.4	n/a	RES-powered electrolysis	n/a
[34]	7.5 - 7.8	125	Wind and PV-powered electrolysis	off-grid
[35]	5.83	125	Wind and PV-powered electrolysis	off-grid
[36]	5.26 - 5.84	938 - 30,000	On-site electrolysis	on-grid
[37]	10.22 - 13.73	50 - 200	PV-powered electrolysis	off-grid
[38]	14.86 - 18.24	100 - 1,000	On-site electrolysis	on-grid
[39]	7.17	4202	Solar on-site electrolysis	on-grid
[40]	4.84 - 6.50	–	Wind and PV-powered off-site electrolysis,	off-grid

[a] Conversion from euros to dollars assumes 1 $ = 1.088 €.

chosen arguably arbitrarily or for the sake of establishing reference data for that region or country that may have been understudied previously. Site-specific studies are reported in [31,34,35,41]. On the other hand, broader perspectives are taken in studies such as [31,40,42,45].

When TEAs regarding HRSs do not consider at any point in their methodology the event-based nature of hydrogen refuelling, both the economical results, e.g., NPC and LCOH values, or the technical results, e.g., dimensioning of hydrogen storage and compressors, implicitly ignore the effects such event-based nature present in the hydrogen demand of HRSs, which should not be considered as any other continuous demand profile of a common energy supply station, e.g., wind farms, nuclear plants or even hydrogen production plants. In HRSs, hydrogen demand is intermittent; the dispensers are either occupied or not. In HRSs, when hydrogen demand is not zero, there are initial and end-point pressure values that affect the dimensioning of the HRSs across all stages (hydrogen supply, compression, storage, cooling); thus, the requirements to satisfactorily refuel multiple FCEVs, specially back-to-back, do not translate to the effects of summing up the absolute value of hydrogen demand during that time period. Thus, when conducting TEAs about HRSs, if there is not a tailored demand aggregation methodology that somehow implicitly considers the event nature of hydrogen demand in HRSs, TEAs on HRSs should build their methodologies with steps that explicitly consider this intermittent demand nature, which is not common in the literature.

Besides how hydrogen demand is considered along the methodology taken in TEAs about HRSs, their gross initial or target values are usually estimated for potential future scenarios. Here, it is a common path to analyse or devise scenarios where ICEVs are replaced by FCEVs in specific vehicle fleets or the overall national grid, as in [40]. In regard to specific fleets, usually public transport fleets are targeted, as can be taxi fleets [13,44] or bus fleets [36]. Specifically, the study conducted in [13] is set in Brazil, where different scenarios of FCEVs market penetration are analysed, and the study presented in [44] is set in Madrid, Spain, where the taxi fleet refuels at off-site HRSs distributed in a 5.5 km radius around the city. In a study set in Brussels, Belgium, a bus fleet is the target demand. In this case, different HRS designs are proposed based on the optimization objective, which targets minimizing carbon intensity or driving cost of the fleet. In terms of minimizing driving cost, 56% of the fleet should be replaced by hydrogen-powered buses. As an example of a simpler approach is that taken in the recent study reported in [39], where a 10% of ICEVs in the region are assumed to be replaced by FCEVs, which are all assumed to have a constant refuelling demand. Other studies apply comprehensive methodologies to forecast hydrogen demand at the targeted future scenario. For example, they may be based on the national traffic census, as in [36] for a 2050 German setting, or an approach that takes into consideration population development, market share, and GDP translation into the number of FCEVs sold for a 2030 Spanish setting, as in [22]. Interesting to note that according to their model, 475,620 FCEVs were estimated to be in circulation by 2030 in Spain. On the other hand, studies such as [46] may take the number of FCEVs from a national roadmap, in this case, Chinese. Recent studies, such as [47], may improve on that by taking into consideration current data on traffic census, population distribution and national roadmaps.

As noted, results of TEAs on HRSs are explicitly dependent on the location of the studied HRSs; thus, several studies have been tackling explicitly or indirectly the allocation/location problem of HRSs to improve the hydrogen infrastructure rollout, both in availability and costs. Across these studies, two main clusters can be differentiated: one using mathematical location models for optimal site selection and the other locating HRS based on existing petrol stations. In a recent review on location strategies [48], three primary models are identified: set covering, p-median (p-mean, and variants) and the Fuel Capture Location Model (FCLM). The FCLM has been utilized in two studies set in Germany, namely, the study conducted in [36] takes a nationwide perspective to locate grid-connected HRSs, and the work reported in [49] locates HRSs under a provider competition setting in Munich. Most recently, FCLM has been utilized in [50] for the Yangtze River Delta region in China. On the other hand, the p-median method is utilized in [51] and, more recently in [47] to locate HRSs in Beijing and Xi'an, respectively. Besides, a common thought is to utilize the existing network of gas/service stations by reconditioning or adapting them to refuel FCEVs. In this regard, the study set in the Netherlands [45] analysed the technical and legal capabilities of existing service stations of placing a wind turbine next to the station to generate electricity for electrolytic hydrogen production. Results showed that only 4.6% of stations fulfil the requirements, which could satisfy 2.3% of the total hydrogen demand in a scenario where 30% of vehicles are replaced with FCEVs. Similarly, the study set in Spain for a 2030 scenario [22], a threshold of Internal Combustion Engine Vehicles (ICEVs) is calculated, indicating how many ICEVs per existing refuelling station need to be refuelled for the service station to be adapted to refuel FCEVs too. The baseline result suggests that 68 out of more than 8000 existing petrol stations should be adapted to allow hydrogen refuelling.

Also common in the literature on TEAs about HRSs is the use of commercial software tools or their combined use with models developed by the authors for areas such as hydrogen demand or techno-economic parameters, as is the case of [36] combining a comprehensive stochastic optimization problem and specific component-level dynamic equations with a commercial software tool for overall HRS dimensioning. In this regard, a widely used software tool is the Hybrid Optimization of Multiple Energy Resources (HOMER) [52], which simulates power systems integrating solar PV systems, wind turbines (WTs), batteries, hydropower and conventional generators. Several studies such as [31,34,35,42,53,54] utilize HOMER, and have served as a methodological reference for this work. Here, it is interesting to note that studies present in the literature may develop their own optimization-based method for HRS design; however, the proposed method does not actually improve or add any significant advantage to justify the avoidance of HOMER for that task. This is the case of the recent study [39]. Hence, when reviewing or proposing a TEAs about HRSs, authors should be aware of the current state of available tools such that the methods proposed actually derive and improve on them if the authors find

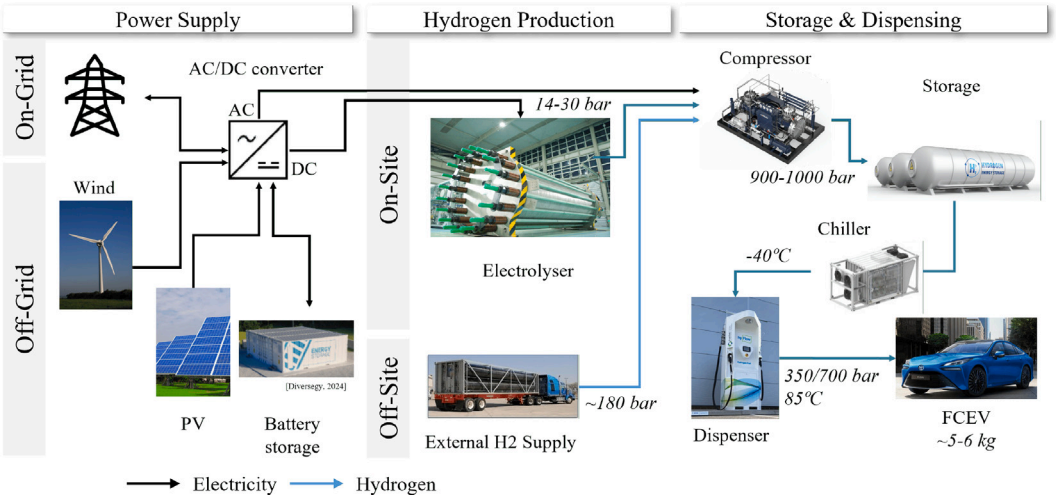

Fig. 1. Diagram of the generalized structure of HRSs.

them lacking or not adequate, but otherwise, researchers conducting TEAs on HRSs should, at least, exploit tools such as HOMER or other freely available tools. Besides, the Hydrogen Refuelling Station Analysis Model (HRSAM) is also frequently used in studies such as [36,44,55], which is developed by the Argonne National Laboratory [15].

For this study, it is pivotal to cite the recent TEA conducted in [40] since it was located in Spain for a 2050 scenario. This study assumes a complete replacement of all vehicles with FCEVs by 2050 and focuses on off-site hydrogen production. The hydrogen production site selection process is centred on seven existing regasification plants repurposed to host hydrogen electrolyzers. The refuelling stations were selected based on the existing network of petrol stations. Two hydrogen distribution methods are evaluated: liquid hydrogen transported by trucks and gaseous hydrogen delivered through the existing natural gas infrastructure, which is already connected to the regasification plants. The HDSAM software developed by the Argonne National Laboratory is employed for the comparison. Spain (excluding the Balearic and Canary Islands) is divided into six regions based on the proximity of regasification plants. Land eligibility is analysed for each region to assess the feasibility of using RES to power the electrolyzers. This analysis is conducted using the GLAES programme. Subsequently, HOMER is employed for techno-economic optimization, determining the optimal system sizing and cost of hydrogen production powered by RES. The study presents results regarding the LCOH for each region and delivery method. On average, gaseous hydrogen supply is found to be 17% cheaper than liquid hydrogen distribution. Their estimated LCOH ranges between 4.84 and 5.99 $/kg for compressed hydrogen gas supply and from 5.99 to 6.50 $/kg for liquid hydrogen supply.

1.3. Contribution

This study aims to foster the development of a comprehensible HRS network across Spain by 2030 that meets the projected hydrogen demand from FCEVs and is coupled with RESs. This HRS network is based on the national Spanish hydrogen roadmap [7], which targets specific objectives such as the number of HD-FCEVs and number of HRSs by 2030. Across the methodology taken in this study, several factors can be highlighted: (a) hydrogen demand is based on real roadmap targets or traffic census data and reliable forecasting studies, (b) the allocation of HRSs also considers the national roadmap and the current network of petrol stations, (c) reported patterns on intra-daily refuelling behaviour is considered, and (d) available trusted tools in the sector are jointly utilized. More specifically, this study does not assume a complete replacement of the Spanish vehicle fleet by FCEVs as in [40], but similarly to [40], the Spanish territory is discretized based on RES potential and multiple tools are jointly used, as is the case with HOMER. Additionally, this study defines the per-HRS capacity in blocks of two sizes for each geographical zone. Utilizing the methodology proposed in this work, the intermittent nature of refuelling FCEVs and their effects on the HRS sizing are considered and, additionally, optimization-based methods are employed for other HRS aspects, as RESs, on-site electrical storage and electrolysis production or grid-interaction. Additionally, this study analyzes both grid-connected and off-grid topologies for the proposed national network. This study has the objective of establishing a base guideline on the requirements and expected costs of the proposed national roadmap, as well as a methodology between the common methods in the literature sectors that mainly focus on specific aspects, such as HRS allocation, techno-economics or optimal sizing. Moreover, this study presents a methodology that can be easily applied to other locations and built upon, similar to that of [40].

2. Hydrogen refuelling stations

Hydrogen refuelling stations fall into two primary categories: on-site and off-site. In on-site stations, hydrogen production occurs directly at the refuelling facility, while in off-site stations, hydrogen is centrally produced and then transported to the refuelling station. Hydrogen is usually transported in trucks in gaseous or liquid form or via pipelines as gaseous hydrogen [1,30]. Furthermore, HRS can be classified based on their grid connection: on-grid HRS are linked to the electrical grid for either drawing or selling electricity, whereas off-grid HRS operate independently [30,56].

Fig. 1 depicts the structure of an HRS. Electricity may be sourced from one out of four sources: a Wind Turbine (WT), a PV system, or the power grid. The electrolyzer utilizes the generated electricity to produce hydrogen. Electricity can be drawn from the grid to the electrolyzer or an electrochemical battery for later use in higher-priced periods or during higher electrical loads that may surpass the grid connection point design limits. In electrolyzers, water is split into hydrogen and oxygen through water electrolysis. The hydrogen produced is generally in a low-pressure gaseous state, usually under 35 bar, and needs to be compressed further for efficient storage. Compressors raise the hydrogen pressure to the required levels, which may vary in HRS designs. Then, the compressed hydrogen is stored in tanks until it is needed to refuel FCEVs. During the refuelling process, the temperature of the gas inside the FCEV onboard tank increases, a fact that justifies the existence of a cooling system to prevent overheating and safely dispense the hydrogen gas to the FCEV [30,56].

2.1. Power supply

The most common types of RES used to produce renewable hydrogen are wind and solar PV. The selection of the RES sources affects the resulting costs. In this aspect, according to [57], the LCOH is higher for hydrogen produced by PV-powered electrolysis, valued at 9.49 $/kg, than from wind-powered electrolysis, valued at 5.61 $/kg.

Wind turbines

Wind energy is generated by transforming the wind's kinetic energy into mechanical energy of a wind turbine, which is then converted into electrical energy using a generator [58]. Depending on the location and application, wind turbines can vary in size. In recent years, onshore wind turbines for grid electricity generation are becoming taller, with hub heights between 80 and 130 m and blades of up to 10 to 80 m of length [59–62]. The power curve is a function that shows the power output depending on the wind speed and is usually provided by the manufacturer. Common modern onshore wind turbines have a capacity between 1 and 4 MW [61,63]. Wind turbines can only produce power between a minimum and a maximum wind speed specific to its hub height, defined by the power curve. Wind speed is usually measured by weather stations at 10 m above the ground. However, wind speed increases with height. Therefore, the wind speed at the hub height of the wind turbine needs to be calculated. Wind turbines usually have a service life of 20 to 30 years [59,63,64].

Solar photovoltaic energy

Photovoltaic energy is produced when sunlight is absorbed by a semiconductor material, causing its electrons to become excited and generate an electric current when connected to a load. Photovoltaic panels consist of multiple solar cells, typically made of several thin layers of semiconductor materials such as silicon. When sunlight strikes the solar cell, photons transfer their energy to electrons, which flow through the semiconductor material as Direct Current (DC) [65]. The DC generated by a PV-panel usually is converted to an Alternating Current (AC) by using a power converter to inject it into the utility grid. Any excess electricity can be stored in a battery during peak sun hours or sold to the grid [13,66]. PV panels are usually measured by their capacity in kW. PV systems are highly flexible and available in a wide power range. This is made possible by connecting the panels in series or parallel to obtain the desired capacities [67]. The expected lifespan of PV systems is about 25 years [13,66].

2.2. Hydrogen generation

There are different ways to obtain hydrogen, usually classified into grey, blue and green hydrogen [11]. Grey hydrogen refers to hydrogen produced from fossil fuels, such as natural gas, through Steam Methane Reforming (SMR). This process emits carbon dioxide (CO_2) as a byproduct, contributing to Greenhouse Gas (GHG) emissions [11]. Blue hydrogen is produced similarly to grey hydrogen, using fossil fuels, with the distinction of mitigating CO_2 emissions through CCUS technologies. On average, SMR accounts for 9.26 $kgCO2eq/kg_{H_2}$, whereas SMR with CCUS, the emissions can be reduced to 1.03 $kgCO2eq/kg_{H_2}$ [57]. Hydrogen produced by SMR is the cheapest hydrogen with an LCOH of 1.2 to 2.1 $/kg [68,69]. Green hydrogen is produced using methods that cause few to no GHG emissions. To qualify as green hydrogen, the emissions produced by the production process must be less than 70% of the reference grey hydrogen production technology, SMR. As stated by the association Hydrogen Europe [70], green hydrogen can produce a maximum of 3.38 $kgCO2eq/kg_{H_2}$ and it is only attributed to the electricity consumed for hydrogen production from the utility grid mix. The most common green hydrogen production method is water electrolysis powered by RES. Electrolysis occurs in an electrolytic cell, which consists of two electrodes, an anode and a cathode, separated by an electrolyte [11]. Multiple electrolytic cells can be combined into an electrolyzer stack, then integrated into a module. Finally, multiple modules comprise an electrolysis system [64,71]. This hierarchical design allows for the customization of electrolysis systems to meet specific demands, achieving capacities of up to 100 MW [72]. The rated capacity of an electrolyzer indicates the maximum amount of electrical power that the electrolyzer consumes at any given moment to produce hydrogen [64,72]. After the electrochemical water-splitting process, hydrogen gas is collected at the cathode and can be captured and stored. In contrast, oxygen gas is collected at the anode and released or stored [13,68,73]. Electrolyzers typically have an efficiency of 60 to 80% , which refers to the ratio of the energy content of the produced hydrogen to the electrical energy input required to perform the electrolysis process [73]. There are different types of electrolysis. The most common and advanced types are the alkaline water electrolysis and the Polymer Exchange Membrane (PEM) electrolysis [11, 31,73]. In an alkaline electrolyzer, an alkaline solution is used as the electrolyte, typically consisting of potassium hydroxide (KOH), whereas in PEM electrolysis, a solid proton-conducting polymer is used as the electrolyte. Other types of electrolysis include the Anion Exchange Membrane (AEM) water electrolysis, which does not require precious metals, and the solid oxide electrolysis, with ceramic materials as the electrolyte. Most of these options present lower costs than PEM electrolysis but require further development to reach commercial viability [7,11].

2.3. Storage and dispensing

Hydrogen storage and compression present significant challenges due to the low density of hydrogen gas [31]. Two main methods are used to increase hydrogen pressure for refuelling the FCEV onboard tanks at 350 and 700 bar: cascade systems and booster compressors. An exhaustive study on perceived hydrogen costs under different assumption scenarios establishes a delivery hydrogen pressure of 700 bar as the lowest cost option for a regionwide FCEV adoption, as well as the most appropriate for an initial market state [74]. After compression, hydrogen is stored in high-pressure storage tanks until it is delivered to the vehicles. The capacity of hydrogen storage is defined by pressure, volume or mass. Usually, multiple tanks are combined, mainly if cascaded storage is used. The size of the individual storage tanks can vary depending on the desired storage capacity and the desired size of the HRS, which is why the costs are often indicated as cost per kg. Hydrogen stored in high-pressure tanks in the 500 to 900 bar range must be expanded to the desired hydrogen dispensing pressure of 350 or 700 bar [11,75–77]. As hydrogen has a negative Joule-Thomson coefficient at room temperature, its temperature increases during an isenthalpic expansion. Consequently, the gas must be pre-cooled before dispensing it to the FCEV onboard tanks. According to the SAE J2601 refuelling protocol, the temperature of the FCEV onboard tank should not exceed 85 °C during refuelling [11,13,30,75]. Hydrogen dispensers monitor and control the refuelling process of hydrogen from the storage tanks or compressors to the FCEV onboard tanks. The dispenser consists of a hose, nozzle, and other electrical complements [30,77]. Other additional components in HRSs may encompass control, data acquisition, communication and safety systems. Additionally, in HRSs coupled with RES such as the one depicted in Fig. 1, power converters and electrical energy storage systems might be part of the HRS design [30,34,35,41]. Power converters may encompass inverters when converting DC to AC, e.g., to supply PV surplus to the grid. On the contrary, rectifiers are required when converting AC to DC, e.g., when feeding the electrolyzers from a standard AC grid or wind turbines [52].

3. Methodology

This study evaluates the techno-economic challenge of deploying a nationwide network of RES-based HRSs in Spain by 2030. The methodological approach comprises the following steps:

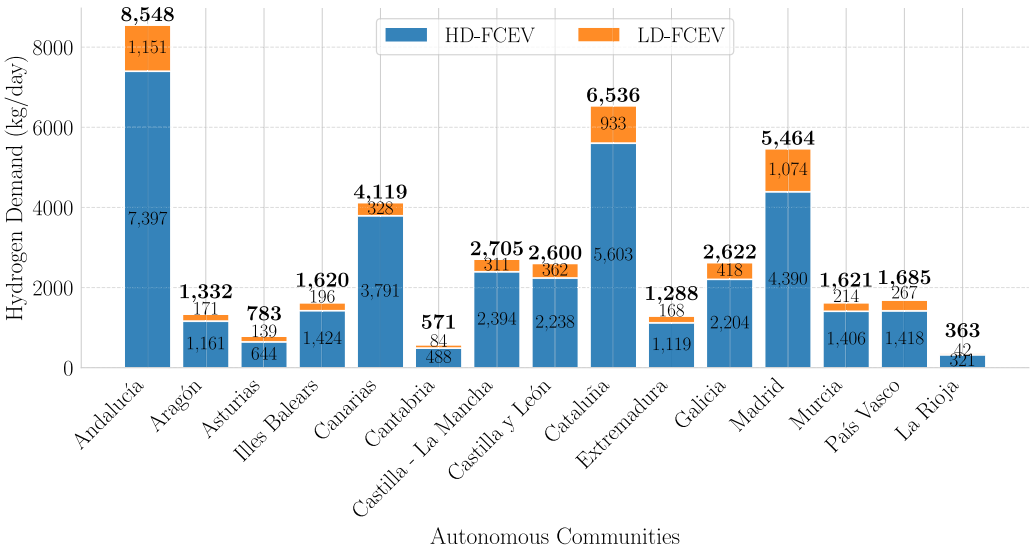

Fig. 2. Daily hydrogen demand for LD- and HD-FCEVs per Autonomous Community.

1. Group Spain's 17 Autonomous Communities (ACs) into five geographical zones/clusters regarding the yearly solar irradiation and wind speed averages, and derive representative monthly renewable energy profiles for each zone.
2. Estimate the 2030 hydrogen demand per province by defining separate numbers of LD- and HD-FCEVs based on the Spanish government's 2030 mobility targets and the current available ICEVs fleet data.
3. Allocate a preliminary number of HRSs among all provinces proportionally to their share of existing petrol stations.
4. Define two HRS daily capacities, small and large, for each RES-zone (grouping the Balearic and Canary islands) by solving a mixed-integer quadratic-constrained optimization problem. The solution determines their optimal capacity (also referred to as *size*) and their allocation across each province that meets local demand and minimizes excess hydrogen capacity and HRS units. This HRS distribution takes into account the preliminary result from the previous step.
5. Perform a techno-economic modelling of the small and large HRSs under both on-grid and off-grid scenarios by integrating outputs from multiple tools and manual calculations to evaluate all key components present in the proposed renewable HRS network.
6. Analyse the overall network based on NPCs and LCOH for each RES-zone and on-grid/off-grid topologies, identifying the most cost-effective configurations and clarifying the impact of the grid.
7. Assess the emissions impact of the HRS network.

3.1. Hydrogen demand estimation

Hydrogen demand is calculated for the 17 Autonomous Communities (ACs) and their 50 provinces, excluding Ceuta and Melilla, on the premise that demand scales with the projected fleet of FCEVs, which are estimated differently for LD- and HD-segments.

However, forecasts regarding the future FCEV market remain highly variable, as illustrated in Table 1. This variability stems from the inherent uncertainties in the penetration of a new powertrain technology into a sector dominated by internal combustion engines for over a century. The evolution of the FCEV market will therefore be strongly influenced by policy decisions and by the competitiveness of alternative technologies, particularly BEVs and hybrids. As a result, the Spanish fleet estimations considered in this work, especially for LD-FCEVs, should be understood as scenario-based inputs subject to such uncertainties. Thus, there exists the possibility of either over- and under-estimation of the demand values, depending on future developments. Furthermore, achieving the assumed 2030 scenario would likely require strong policy measures to actively foster FCEV adoption, particularly in the LD segment, as has already occurred for BEVs in several European countries.

National fleet in 2030. The Spanish Hydrogen Roadmap anticipates 7500 fuel-cell trucks and 200 fuel-cell buses by 2030 [7], thus, a total 7700 HD-FCEVs. In the light-duty segment, the Hydrogen Council foresees 4.2 million LD-FCEVs across Europe by 2030 [18]. Spain's present share, 23 of 5503 vehicles [16], amounts to 0.4%. Applying this fraction gives 17,554 LD-FCEVs in Spain by 2030, which is the value assumed in this study.

Regional allocation. Projected national totals are distributed to each province in line with the 2022 distribution of ICEVs [78].

Light-duty demand. Refuelling behaviour is assumed to mirror that of conventional cars. A BP survey of Spanish drivers [79] gives a weighted average of 2.53 refuelling events per month, which aligns with the results reported in [80]. With an assumed average fill of 4.5 kg, this yields the daily light-duty demand in each province once scaled by its projected LD-FCEV population and the refuelling frequency. Demand is spread evenly across the month to obtain daily values for each province.

Heavy-duty demand. Empirical data for fuel-cell buses reported in [81] provides a basis for the heavy-duty segment. The study records an average consumption of 7 kg per 100 km and a typical fill of 14.63 kg, equivalent to one stop every 209 km. Annual driving distances in Spain, 49,276 km for trucks and 26,765 km for buses [82], are combined in proportion to the 2030 national HD-FCEV fleet objective, giving a representative annual mileage of 27,308 km per HD-FCEV, assumed constant for all provinces. Demand is spread evenly across the year to obtain daily values for each province.

National result. The methodology taken in this study yields a hydrogen demand of 6651 kg/day for LD-FCEVs and 40,857 kg/day for HD-FCEVs, a combined 47,509 kg/day nationwide. Fig. 2 presents the hydrogen distribution by AC.

Intra-day profile. Hydrogen refuelling stations are considered open from 06:00 h to 23:00 h. Hourly demand is considered a function of the HRS capacity (daily throughput), represented by an hourly share/weight. Hourly demand in each RES-zone (Section 3.3) is a weighted blend of two base patterns, namely, the hourly distribution of LD-FCEV refuelling events reported in [80] and the mean hourly share of heavy-duty refuelled mass compiled by Caponi et al. [81]. After

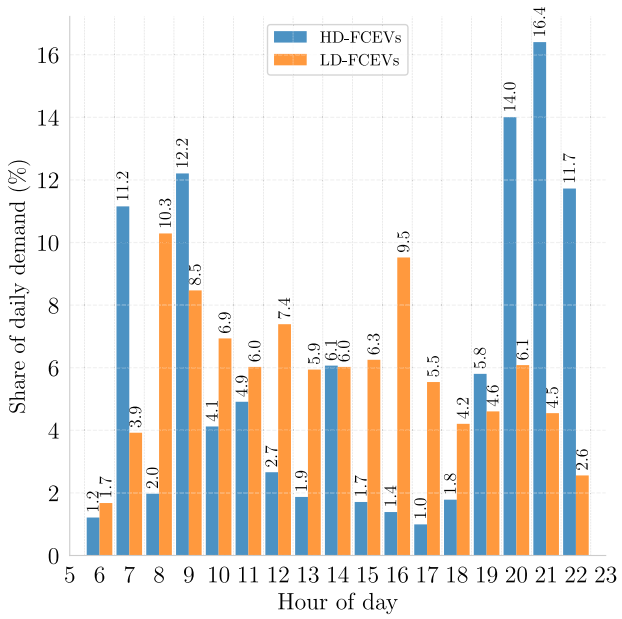

Fig. 3. Base hourly share of daily demand for LD-FCEVs, derived from [80] and HD-FCEVs, derived from [81].

discarding closed hours, both patterns are renormalized to 100% and they are depicted in Fig. 3. Weights correspond to the LD/HD shares listed in Table A.11. The resulting zone-specific average fill per vehicle, needed by HDRSAM, is the weighted mean of 4.5 kg for LD-FCEVs and 14.63 kg for HD-FCEVs, weighted in terms of the fleet of HD/LD-FCEVs in each RES-zone, the same approach as in the refuelling pattern.

3.2. HRS sizing and distribution

The distribution of HRSs across Spain builds upon the existing network of 11,711 petrol stations [83]. Specifically, each province is initially assigned a minimum number of HRSs proportional to its share of national petrol stations, ensuring territorial equity. To determine these provincial minimum quotas, an illustrative allocation of 75 stations was distributed according to provincial petrol-station shares. The number 75 was selected by trial and error, as it is the smallest integer that, when proportionally allocated and rounded at the provincial level, sums up to 99 HRSs nationally, just below the minimum national target of 100 HRSs established by Spain's Hydrogen Roadmap [7]. The details of this initial allocation, including petrol-station shares per province and the resulting minimum HRS quotas, are presented in Table A.12.

In terms of station sizing, the literature typically classifies HRS capacities into three broad and loose-defined categories: small stations (100 kg/day to 150 kg/day), medium-sized stations (450 kg/day to 730 kg/day), and large stations (over 1000 kg/day) [30,36,56]. For simplicity, this study considers two discrete station sizes, defined as the *Small HRS* and *Large HRS*. Here, the term *capacity* or *size* strictly refers to daily hydrogen dispensing capability, excluding considerations of on-site hydrogen production (daily hydrogen production capacity can be higher than its target daily refuelling capacity).

This work optimizes distinct capacities for each RES-zone (see Section 3.3), considering that the Canary and Balearic islands are in the same zone, referred as *Islands*. Specifically, each RES zone z has its own integer capacities for small stations, c_S^z, bounded between 100 and 300 kg/day, and large stations, c_L^z, bounded between 400 and 900 kg/day.

The objective of the optimization is twofold: first, to minimize the total number of HRSs deployed, and second, to minimize any surplus dispensing capacity above provincial hydrogen demands. Let

Table 3
Optimal HRS capacities per RES zone.

RES Zone	Small HRS capacity (kg/day)	Large HRS capacity (kg/day)
Central	122	408
Islands	236	816
North	165	406
South	128	548

$x_{S,i}$ and $x_{L,i}$ denote the integer numbers of *Small* and *Large* stations allocated to province i, respectively, whose daily hydrogen demand is d_i. Province i is associated with RES-zone z_i. Due to bilinear terms arising from the multiplication of station counts and capacities, the resulting optimization problem formulated is in the family of Mixed-Integer Quadratic-Constrained Problems (MIQCPs), known to be especially hard to solve:

$$\min_{\substack{x_{S,i},x_{L,i}\in\mathbb{Z}_{\geq 0}\\ c_S^z,c_L^z\in\mathbb{Z}}} \sum_i \left(x_{S,i}+x_{L,i}+x_{S,i}c_S^{z_i}+x_{L,i}c_L^{z_i}-d_i\right) \tag{3.1a}$$

$$\text{s. t.}\quad x_{S,i}c_S^{z_i}+x_{L,i}c_L^{z_i}\geq d_i,\quad \forall i, \tag{3.1b}$$

$$x_{S,i}+x_{L,i}\geq S_i,\quad \forall i, \tag{3.1c}$$

$$100\leq\sum_i(x_{S,i}+x_{L,i})\leq 150, \tag{3.1d}$$

$$100\leq c_S^z\leq 300,\quad \forall z, \tag{3.1e}$$

$$400\leq c_L^z\leq 900,\quad \forall z. \tag{3.1f}$$

Eq. (3.1a) minimizes both the total number of stations and surplus dispensing capacity above provincial demand. Ineq. (3.1b) ensures each province's hydrogen demand is satisfied, while Ineq. (3.1c) ensures provincial minimum quotas S_i are respected, reflecting petrol-station distribution. Ineq. (3.1d) imposes national limits on the total number of stations, and box constraints (3.1e) and (3.1f) restrict HRS capacities to stay within realistic ranges.

The MIQCP was formulated in AMPL [84] and solved using Octeract solver [85], a global optimization solver utilizing convex relaxations and branch-and-bound methods suitable for bilinear terms. To keep computational efforts manageable, the solver runtime was limited to 16 h. At termination, an incumbent solution that satisfies all constraints with minimal cost was retrieved. Optimal capacities for each RES-zone as provided by the solver are summarized in Table 3. The optimal solution distributes a total of 149 HRSs nationwide; the exact provincial distribution is detailed in Table A.13 and visually represented in Fig. 10. Interesting to note from Table 3 how the Islands capacities per station, either Small or Large, are significantly higher than in other zones. This is potentially due to a lower density of petrol stations in such areas, which leads the optimizer to minimize the absolute number of stations, compensating for the demand fulfilment by allocating higher capacities to each type.

3.3. Renewable potential zones

By dividing Spain into zones based on their renewable energy potential, the nationwide TEA becomes more manageable and provides a broadened understanding of regional patterns. To evaluate the solar irradiation, the Global Horizontal Index (GHI) is measured in kWh/m^2/day, representing the total solar energy received on one square meter over one day [86]. Wind speed and solar irradiation data were obtained from NASA's Prediction Of Worldwide Energy Resources (POWER) [87]. For each of the 50 provinces,[1] average daily

[1] Excluding Ceuta and Melilla.

Table 4
Mainland RES zones breakdown by Autonomous Communities.

Mainland RES-zone	Autonomous Community (AC)
South	Extremadura Andalucía Región de Murcia Comunitat Valenciana Comunidad de Madrid Castilla-La Mancha
Central	La Rioja Aragón Cataluña Castilla y León Comunidad Foral de Navarra
North	Galicia Cantabria País Vasco o Euskadi Principado de Asturias

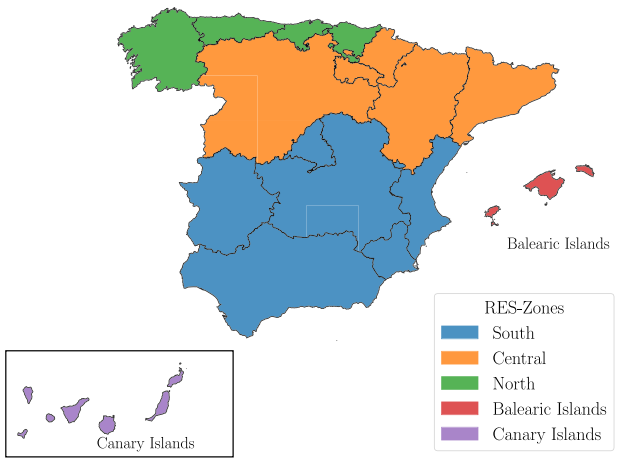

Fig. 4. Map of Spain according to the RES-zones.

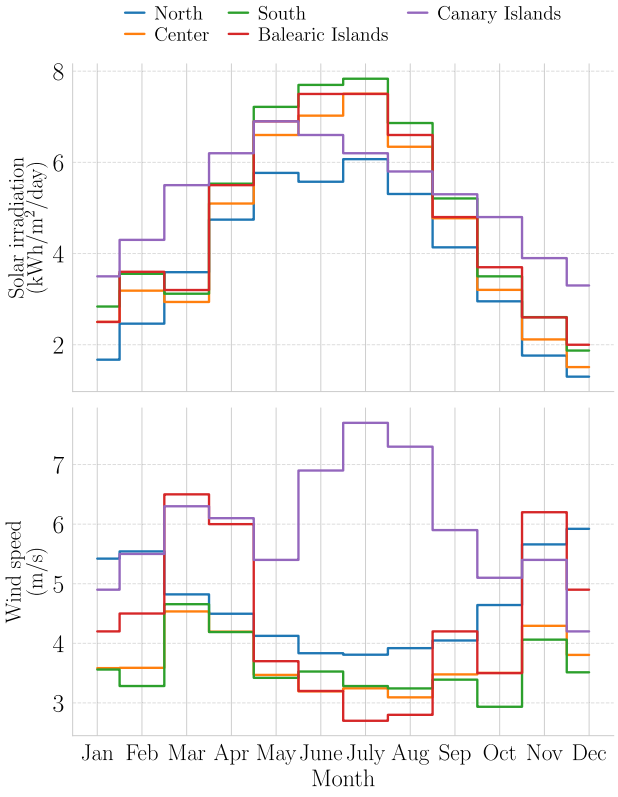

Fig. 5. Monthly average solar irradiation and wind speed (at 10 m) across different RES-zones.

values are provided for every month of the year. Consequently, the monthly average solar irradiation is reported in kWh/day, and the average daily wind speed, measured at a 10 m anemometer height, is given in m/s. The authors are aware of the simplicity of the proposed approach, specifically critical regarding wind generation, as it is location-dependent, and many locations are not suitable for a WT setup. Nonetheless, this is a first approach that can capture RES potential variation across the country.

The following procedure was employed to categorize the mainland ACs into *RES-zones*. Monthly values for each province were averaged to obtain the corresponding monthly values for each mainland AC. These monthly values were then averaged across the year to calculate a yearly average value for each AC. Based on these annual averages, AC were grouped into three mainland zones with similar values (see Fig. 4 and Table 4). Finally, for each zone, the average monthly values were calculated by averaging the respective communities monthly values within the zone. In regard to the islands, they present different averaged profiles and are treated separately with the same approach, their averaged solar irradiation and wind speed profiles are depicted in Fig. 5. Specifically, it can be noticed that South Spain has the highest average yearly solar irradiation, with 4.9 $kWh/m^2/day$, and the lowest wind speed, at 3.58 m/s. Central Spain experiences an intermediate solar irradiation of 4.39 $kWh/m^2/day$ and a wind speed of 3.67 m/s. In contrast, North Spain has the lowest solar irradiation at 3.78 $kWh/m^2/day$, but the highest wind speed at 4.68 m/s. Across all zones, the highest solar irradiation values occur in summer, while wind speeds are typically higher in winter. In the Balearic Islands, the average annual solar irradiation is 4.7 $kWh/m^2/day$, with an average annual wind speed of 4.4 m/s. The Canary Islands have an even higher solar irradiation of 5.2 $kWh/m^2/day$ and a wind speed of 5.9 m/s, higher during summer, contrary to other RES-zones.

The breakdown of the mainland RES-zones per AC is presented in Table 4 and at the province level can be found in Table A.13.

3.4. Techno-economic modelling

This section describes the techno-economic modelling strategy developed to evaluate the deployment of a national HRS network. The selected methodology must comprehensively account for both capital and operational costs associated with hydrogen production, electricity consumption, renewable energy integration, and hydrogen demand. To this end, several modelling tools commonly used in the literature were examined based on their capabilities and limitations.

Among the available tools, HOMER is particularly relevant in the literature, as it enables optimization of systems powered by various energy sources (grid, PV, wind) to meet an electric load. These loads may represent the electricity consumed by an electrolyzer to produce hydrogen, which is stored and later consumed by hydrogen load. HOMER supports the definition of hourly electric and hydrogen demand profiles, with options for adding seasonal and stochastic variability. The tool performs component sizing optimization, estimates Net Present Cost (NPC), annualized costs, and provides sensitivity analysis features. However, HOMER lacks modelling of key HRS components such as compressors, chillers, and dispensers, ignores pressure dynamics in the sizing of hydrogen storage and FCEVs demand satisfaction, and omits several cost categories like labour, land, permitting, and insurance.

In contrast, the HRSAM, HDSAM, and HDRSAM family of models focus on detailed HRS-specific TEA. These tools incorporate industry-sourced default parameters and consider explicit modelling of subsystems such as buffer and cascaded hydrogen storage, compression,

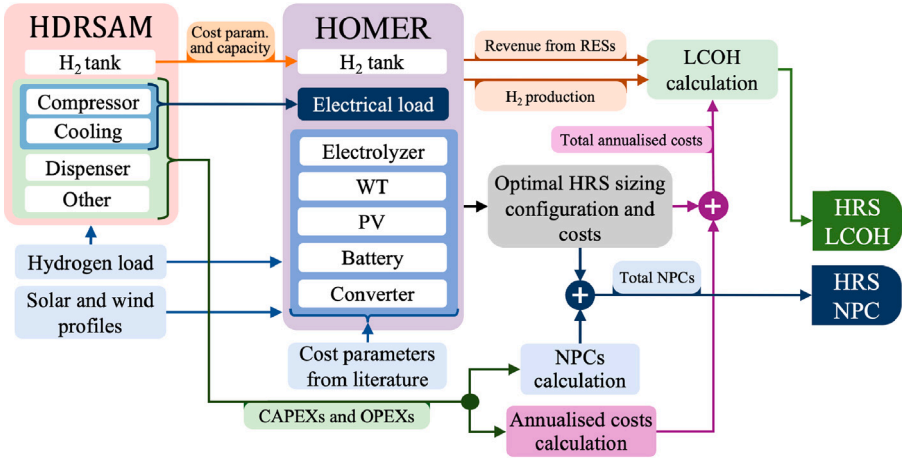

Fig. 6. Diagram of the methodology for the techno-economic modelling approach.

Table 5
Software requirements.

Tool	Requirements			
	Hydrogen Production	All HRS Components	RES	Cost analysis
HOMER	x		x	x
HRSAM,HDSAM,HDRSAM		x		x
H2A	x			x
H2A-Lite	x		x	x
H2FAST				x

cooling, and dispensing. HDRSAM, in particular, includes updated 2022 cost parameters and supports custom hourly hydrogen demand profiles, pressure and volume calculations for storage sizing, energy estimates for compression and cooling, and gaseous HRS topology with buffer storage and cascaded refuelling. This topology is especially flexible for 350 and 700 bar refuelling via electrolysis-based local hydrogen production, aligning with the design of the TRE2103000 project [88,89], in which the authors are involved.

Alternatively, production models such as H2A and H2A-Lite offer detailed insight into hydrogen production costs but lack downstream modelling of HRS components. While H2A provides granular input flexibility, and H2A-Lite introduces some RES integration, both remain limited to production scope and do not capture station-level dynamics. For this reason, they are not used directly but are included in the analysis.

Table 5 provides a qualitative comparison of selected tools based on key criteria: hydrogen production modelling, full HRS component modelling, RES integration, and cost analysis. From this comparison, a hybrid approach using HOMER and HDRSAM emerges as the most comprehensive. While HDRSAM addresses system-specific operational dynamics, HOMER captures system-wide energy flows and economic optimization under variable renewable generation.

The proposed methodology thus combines HOMER and HDRSAM in a complementary manner, leveraging HOMER's optimization of hybrid energy systems and HDRSAM's fidelity in modelling HRS-specific components. A general visualization of the overall methodology is depicted in the diagram of Fig. 6. This dual approach is rarely adopted in the literature.

Taxation of any kind (property, regional, or national) is excluded from the economic analysis. HDRSAM simulations adopt a fixed gaseous HRS configuration with a 20-bar supply pressure and 700-bar cascaded refuelling architecture using two dispensers. These design features remain constant across RES zones and HRS sizes.

Annual HRS utilization is assumed to be 100% over a 25-year service life. Aside from taxes, other secondary parameters are left to default values. Only CAPEX and OPEX results (dated to 2022), along with component capacities and energy demands, are extracted from HDRSAM. These values are integrated differently across the techno-economic modelling pipeline.

HDRSAM allocates fixed OPEX (insurance, permits, G&A) proportionally across HRS subsystems based on their CAPEX share. Therefore, the OPEX values output for compressors, chillers, dispensers, and electrical systems already include a share of these fixed costs. Labour and land-related costs, however, are reported separately.

Regarding hydrogen storage, HDRSAM models both low-pressure and cascaded configurations. Each capacity is computed by incrementally aggregating base units until operational feasibility is achieved. Table 6 reports CAPEX per kg for each subsystem. While cascaded storage results are constant across all cases (80 kg), low-pressure storage varies with HRS size and daily demand, with the Islands Large HRS reaching the highest value. OPEX values shown in Table 7 also reflect this tendency, although slight variations in per-unit costs are due to the CAPEX-weighted cost allocation described earlier.

To incorporate hydrogen storage into HOMER, an aggregate value is used. Averages across the configurations in Tables 6 and 7 yield 2141.20 $/kg CAPEX and 92.52 $/kg/year OPEX, applied uniformly to all HRS sizes in all RES-zones.

From HDRSAM, daily energy demands from compressors and chillers (see Table 8) can be extracted (assuming the annual value obtained is spread evenly each day). These loads are assumed to follow the same intra-daily hydrogen demand profile of each RES-zone, as discussed in Section 3.1, and incorporated as hourly variable electric loads in HOMER.

Additional CAPEX and OPEX entries from HDRSAM that cannot be represented in HOMER are listed in Table A.14. These are included in the overall techno-economic evaluation by computing their annualized and NPC values separately (see Section 3.4.1).

Each HOMER simulation evaluates both on-grid and off-grid scenarios for all HRS sizes and zones. The configuration includes an electrolyzer, hydrogen storage, PV, WT, power converter, and battery. HOMER selects among combinations of these based on economic and

Table 6
CAPEX parameters for storage components by zone-size code, results from HDRSAM. Codes: SS = South Small, SL = South Large; NS = North Small, NL = North Large; IS = Islands Small, IL = Islands Large; CS = Central Small, CL = Central Large. C-HST: cascaded hydrogen storage tank; LP-HST: low-pressure hydrogen storage tank.

Zone Size	Type	Capacity (kg)	CAPEX (2022)	CAPEX (2025)	CAPEX ($/kg, 2025)
SS	C-HST	80.29	161,193	181,664	2,262.46
SS	LP-HST	123.92	222,099	250,305	2,019.92
SL	C-HST	80.29	161,193	181,664	2,262.46
SL	LP-HST	247.84	444,198	500,611	2,019.92
NS	C-HST	80.29	161,193	181,664	2,262.46
NS	LP-HST	123.92	222,099	250,305	2,019.92
NL	C-HST	80.29	161,193	181,664	2,262.46
NL	LP-HST	247.84	444,198	500,611	2,019.92
IS	C-HST	80.29	161,193	181,664	2,262.46
IS	LP-HST	123.92	222,099	250,305	2,019.92
IL	C-HST	80.29	161,193	181,664	2,262.46
IL	LP-HST	371.75	666,296	750,916	2,019.92
CS	C-HST	80.29	161,193	181,664	2,262.46
CS	LP-HST	123.92	222,099	250,305	2,019.92
CL	C-HST	80.29	161,193	181,664	2,262.46
CL	LP-HST	247.84	444,198	500,611	2,019.92

energetic feasibility. Up to four components (PV, WT, electrolyzer, and battery in this study) capacities are continuously optimized in $\mathbb{R}_{\geq 0}$; others, such as the converter, follow a user-defined search space (see Table A.15 for the assumption in this study). Moreover, all on-grid configurations are parametrized with a 1 MW upper limit in selling power capacity to the utility grid. This is intended to minimize potential tendencies of the optimizer in considering the HRS as an electrical energy supply for the grid.

Techno-economic parameters are summarized in Table 9, derived from HOMER defaults and literature [35,42], including external reports [90]. Key financial assumptions include a 25-year lifetime, 2.3% inflation [91], and an 8% discount rate [12,34–36,41].

Hourly electricity prices from Spanish market operators are included using 2023 time series [92,93].

Finally, HOMER's wind turbine model is adjusted to use the power curve and hub height of a commercial 800 kW E-53 ENERCON unit [35], replacing the default 1 kW unit power curve. To be consistent with the hub-height of 73 m, although the WT capacity is optimized in $\mathbb{R}_{\geq 0}$, a lower limit is imposed at 800 kW to resemble that of the base ENERCON model, the upper bound is left in a sufficiently high value such that the capacity is not clipped by the optimizer. Regarding the electrolyzer, the generic model is used, which assumes a 39.4 kWh per kg of hydrogen conversion. The battery considered is the 1 kW lithium-ion [ASM] model, and the PV system is assumed to be the generic flat-plate model. Specific information of the models and optimizer is provided by HOMER [94]. Important to note that HOMER replaces the battery when a degradation threshold is surpassed, in this case 30%. For PV modelling, HOMER requires clearness index data. Since this study works with zonal averages, a representative city is selected for each RES-zone regarding the clearness index: Sevilla (South), Zaragoza (Central), San Sebastián (North), Palma de Mallorca (Balearic Islands), and Las Palmas de Gran Canaria (Canary Islands).

3.4.1. Net present cost and annualized costs

The Net Present Cost (NPC) is a key measure of financial viability that accounts for all project costs over its lifetime while adjusting future expenditures by considering the value change of money over time [34,42,95]. The NPC represents the present value of all costs of installing and operating a component over the project lifetime, minus the present value of all revenues that it earns over the project lifetime. The NPC of the project, C_{NPC}, is the result of the summation of the total net present value of expenses of all components, given by

$$C_{\text{NPC}} = \sum_{k \in \mathbb{E}} C^{k}_{\text{NPC}}, \tag{3.2}$$

where $\mathbb{E}$ is the list of all components. Consequently, the net present cost of each component is defined by

$$C^{k}_{\text{NPC}} = C^{\text{NP},k}_{c} + C^{\text{NP},k}_{o} + C^{\text{NP},k}_{r} - C^{\text{NP},k}_{s} \quad \forall k \in \mathbb{E}, \tag{3.3}$$

where the net present values of the multiple expenditures are summed up. Specifically, these expenditures are the capital expenditure (also referred to as CAPEX or investment cost), C^{NP}_{c}, the operation and maintenance expenses (also referred to as OPEX), C^{NP}_{o}, the replacement cost, C^{NP}_{r}, and the salvage income, C^{NP}_{s}. These expenditures are defined in the following paragraphs.

The capital expenditure represents the initial investment cost that occurs at the beginning of the project (year zero), therefore:

$$C^{\text{NP},k}_{c} = C^{k}_{c} \quad \forall k \in \mathbb{E}, \tag{3.4}$$

where C^{k}_{c} is the capital cost of component k. Since this cost occurs at $t = 0$, it is not required to apply a discounting that accounts for the variation of the value of money.

The OPEX consider the discounted cash flow given by the operation and maintenance expenditures of the component along the project lifetime. Following HOMER methodology, OPEX is set to zero during replacement years to avoid double-counting operational costs that are included in replacement expenses. Therefore:

$$C^{\text{NP},k}_{o} = \sum_{j \in \mathcal{J}_k} d_j \, C^{k}_{o} \quad \forall k \in \mathbb{E}, \tag{3.5}$$

where C^{k}_{o} is the annual operation and maintenance cost of each component, $\mathcal{J}_k = \{j \in \{1, \ldots, n\} : j \notin \mathcal{R}_k\}$ represents the set of years excluding replacement years $\mathcal{R}_k$ for component k, and d_j is the discount factor of each year defined as follows:

$$d_j = \frac{1}{(1 + i_r)^j} \quad \forall j \in \{1, \ldots, n\}, \tag{3.6}$$

with i_r being the real annual discount rate given by:

$$i_r = \frac{i_n - i_e}{1 + i_e}, \tag{3.7}$$

where i_n and i_e are the nominal annual discount rate and the expected inflation rate, respectively.

Similarly, C^{NP}_{r} considers the discounted cashflow given by the sum of replacements of each component, assumed to occur only at the end of their respective lifetime, as given by:

$$C^{\text{NP},k}_{r} = \sum_{j \in \mathcal{R}_k} d_j \, C^{k}_{r} \quad \forall k \in \mathbb{E}, \tag{3.8}$$

where C^{k}_{r} is the replacement cost of each component, and the summation is performed only over the replacement years $\mathcal{R}_k$. The replacement years are those within the project lifetime where the component must be replaced due to its lower lifetime, thus, $\mathcal{R}_k$ for component k are determined by the component lifetime L_k, such that $\mathcal{R}_k = \{L_k, 2L_k, 3L_k, \ldots\} \cap \{1, 2, \ldots, n\}$.

Last, the salvage income is obtained assuming the total return on investment at the end of the project lifetime of the residual value of each component. The residual value of each component is assumed to be the residual depreciated value of the component based on the last replacement cost before the end of the project. For this, a linear depreciation within each components lifetime is assumed. Hence, the salvage income is defined as:

$$C^{\text{NP},k}_{s} = \frac{n^{k}_{r}}{n_k} C^{k}_{r} \quad \forall k \in \mathbb{E}, \tag{3.9}$$

where n^{k}_{r} is the residual lifetime of component k at the end of the project and n_k is the lifetime of the respective component.

The annualized costs represent the total costs of the overall system or components independently spread evenly over each year of the project's lifetime. The Capital Recovery Factor (CRF) is used to convert

Table 7
OPEX parameters for total hydrogen storage by zone–size code, results from HDRSAM. Codes: SS = South Small, SL = South Large; NS = North Small, NL = North Large; IS = Islands Small, IL = Islands Large; CS = Central Small, CL = Central Large. THS: Total Hydrogen Storage.

Zone Size	Capacity (kg)	OPEX (2022 $/year)	OPEX (2025 $/year)	OPEX ($/kg/year, 2025)
SS	204.21	17,688.43	19,934.87	97.62
SL	328.13	25,881.49	29,168.44	88.89
NS	204.21	17,688.43	19,934.87	97.62
NL	328.13	25,881.49	29,168.44	88.89
IS	204.21	17,688.43	19,934.87	97.62
IL	452.05	33,299.69	37,528.75	83.02
CS	204.21	17,688.43	19,934.87	97.62
CL	328.13	25,881.49	29,168.44	88.89

Table 8
Daily electrical consumption from HDRSAM by zone–size code. Codes: SS = South Small, NS = North Small, IS = Islands Small, CS = Central Small; SL = South Large, NL = North Large, IL = Islands Large, CL = Central Large.

Zone–Size	Compressor (kWh/day)	Refrigeration (kWh/day)	Total (kWh/day)
SS	624.54	17.77	642.31
NS	804.64	22.91	827.54
IS	1160.64	32.76	1193.40
CS	595.59	16.94	612.53
SL	2673.83	76.08	2749.90
NL	1979.89	56.36	2036.26
IL	4013.06	113.28	4126.34
CL	1991.82	56.64	2048.46

Table 9
CAPEX, Replacement cost, and OPEX for the HRS components used in HOMER.

Component	CAPEX ($/kW)	Replacement ($/kW)	OPEX ($/kW/year)	Lifetime (years)
PV-panel	650	650	10	25
Wind turbine	2000	2000	40	25
Electrolyzer	2000	1500	200	15
Battery ($/kWh)	700	700	0	–
Power converter	600	600	0	10
Hydrogen storage	2141.20	2141.20	92.52	25

present values to equivalent annual payments and is defined as follows:

$$\mathrm{CRF} = \frac{i_r(1+i_r)^n}{(1+i_r)^n - 1}, \tag{3.10}$$

with n being the project lifetime.

Except for the operational and maintenance cost, which requires special treatment due to the zero OPEX in replacement years, all cost components are annualized using the CRF factor. The annualized values are obtained as follows:

$$C_h^{A,k} = C_h^{NP,k}\,\mathrm{CRF} \qquad \forall h \in \{c,o,r,s\} \wedge k \in \mathbb{E} \tag{3.11}$$

Note that this includes the operational and maintenance costs, where $C_o^{A,k} = C_o^{NP,k} \times \mathrm{CRF}$, ensuring consistency with the NPC calculation that excludes OPEX during replacement years.

Accordingly, the total HRS annualized cost is given by:

$$C_A = \sum_{k\in\mathbb{E}} C_A^k, \tag{3.12}$$

where the annualized cost of each component is defined as:

$$C_{\mathrm{A}}^k = C_c^{\mathrm{A},k} + C_o^{\mathrm{A},k} + C_r^{\mathrm{A},k} - C_s^{\mathrm{A},k} \quad \forall k \in \mathbb{E}. \tag{3.13}$$

To obtain the LCOH, the total annualized costs are divided by the total amount of hydrogen produced. The LCOH evaluates the cost of producing hydrogen, calculated by dividing the total costs of the station by the total annual amount of hydrogen produced, M_{H_2}, and, if appropriate, deducting the revenue, R_{Grid}, from selling excess energy back to the grid [32,35,36].

Table 10
Lifetimes considered for the calculation of NPC and annualized costs of HDRSAM cost entries.

Component	Lifetime (years)
Cooling system	15
Compressor	10
Electrical connection	25
Control and safety equipment	15
Dispenser	10
Other	25

Hence, the LCOH is defined as:

$$\mathrm{LCOH} = \frac{C_A - R_{Grid}}{M_{H_2}}. \tag{3.14}$$

Since the NPC and annualized costs calculation is performed for the HDRSAM components and cost categories that cannot be input directly into HOMER, it is necessary to define various techno-economic parameters for these cases. These parameters involve the lifetime and replacement costs, since the CAPEX and OPEX are already obtained from HDRSAM. It is assumed that the replacement costs of the cost entries in HDRSAM is the same as their respective CAPEX, and the lifetimes considered are presented in Table 10. In Table 10, the entry *Other* refers to labour, land and administrative overhead costs. Regarding their CAPEX and OPEX values, recall they are presented in Table A.14.

4. Results and discussion

This section analyzes the techno-economic performance of a renewable-energy-powered HRS network for Spain, focusing on LCOH, NPC, optimal system sizing, and regional renewable utilization.

Fig. 7 compares LCOH and NPC across station sizes, RES-zones, and grid-connectivity options. As expected, NPC rises with both plant size and off-grid operation: larger systems require higher capital outlay, while off-grid designs must oversize their renewable assets to ensure autonomy. Geographically, small HRSs exhibit similar NPC nationwide, whereas large HRSs incur a marked cost penalty in the islands. This fact is a direct consequence of their higher design capacities (Table 3).

Economies of scale are evident in on-grid configurations: larger stations record consistently lower LCOH than their smaller counterparts. Off-grid behaviour diverges: only the large Balearic and northern sites outperform their small equivalents. The grid, therefore, acts as a revenue stream where oversized RESs can export surplus electricity, whereas off-grid systems benefit from leaner designs that minimize absolute curtailment.

LCOH values span 9.56–24.13 $/kg. Northern sites deliver the lowest costs on the mainland, which rely persistently on a hybrid wind and solar energy supply. In contrast, South and Central zones install no WT in on-grid cases, yet must include wind capacity in off-grid cases. Even so, their self-sufficient designs remain more expensive than those of the North. These findings align with [40,57], which also reported the superior competitiveness of wind-driven hydrogen production. Overall,

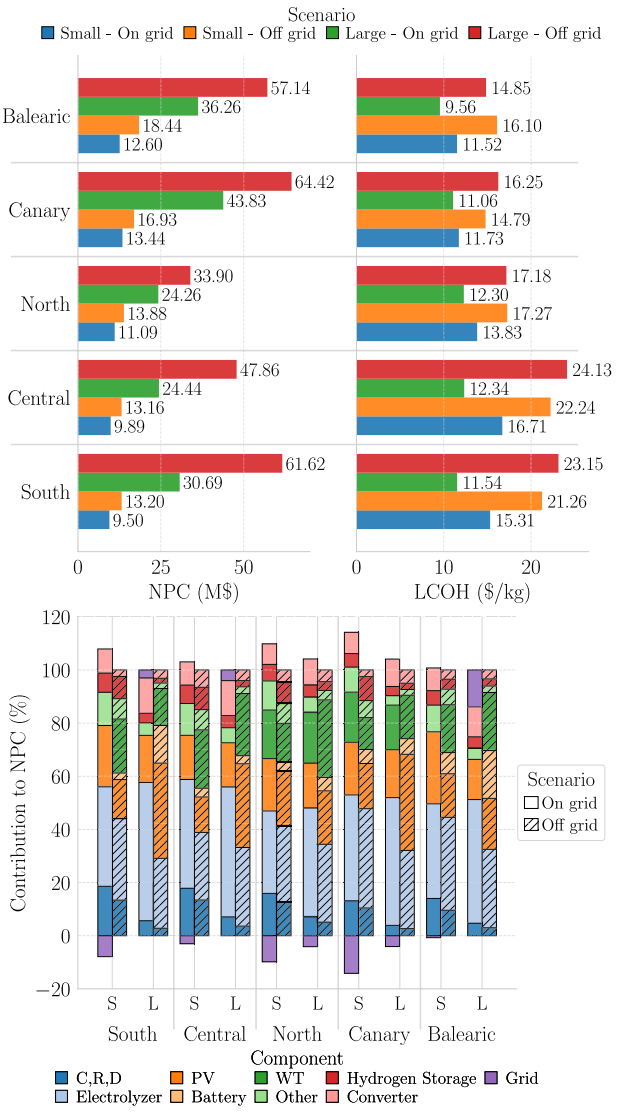

Fig. 7. NPC and LCOH of different HRS configurations (S for Small and L for Large) grouped by RES-zone, and the NPC breakdown by component. Compressor, refrigeration and dispenser costs are referred to as C,R,D, and costs related to land, control and safety equipment, labour and grid connection (only in on-grid cases) are aggregated in the category named Other.

large on-grid HRSs present the most attractive LCOH, and wind power is only warranted in northern regions for that topology.

The Balearic and Canary Islands display comparatively flat LCOH, with relatively limited sensitivity to either station size or grid connection compared to mainland results. Nevertheless, practical constraints, such as land availability and construction logistics, may increase both NPC and LCOH beyond the values reported here.

The NPC breakdowns depicted in Fig. 7 confirm that electrolyzer and RES costs dominate. The grid switches from revenue (negative NPC contribution) to expense in several large on-grid cases, indicating that energy purchases outweigh sales. This effect is most pronounced in the Balearic Islands. Off-grid scenarios, devoid of grid transactions and grid connection CAPEX, exhibit battery costs that rise sharply with size, particularly in the South and Balearic zones. Regarding electrical storage, batteries have been deemed unoptimal for installation in on-grid HRSs. It should be noted that the lowest NPC configurations for all small-sized HRSs, have been found equipped with the large-sized hydrogen storage capacity (see Table 7).

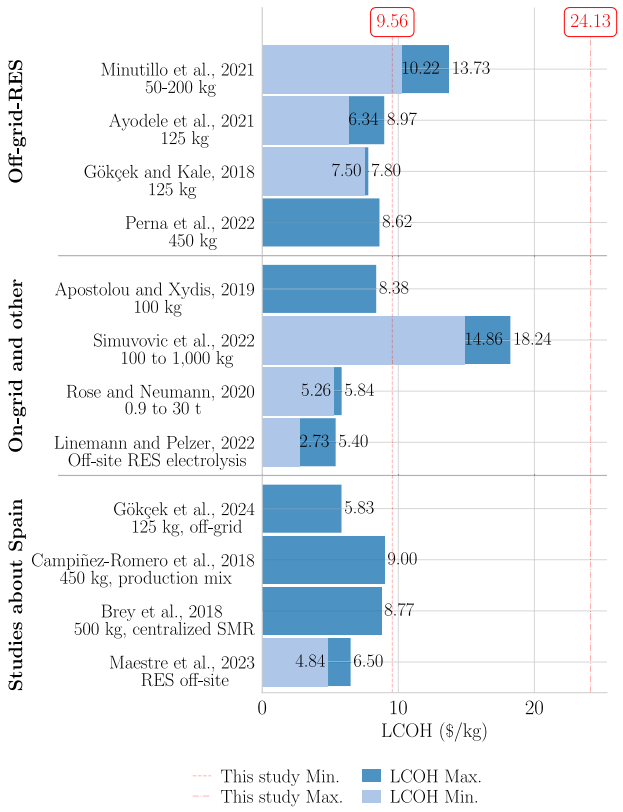

Fig. 8. LCOH comparison with literature results.

Fig. 8 benchmarks our LCOH against literature values. The present study falls within published ranges but generally at the upper end; only two of the displayed studies [37,38] report higher costs attributable to small capacities or restrictive local conditions. Nonetheless, the highest LCOH values reported in this study do surpass any of the literature results referenced in Fig. 8.

For the nationwide roll-out of 149 HRSs, total capital investment is 1.52 G$ (all on-grid) and 3.14 G$ (all off-grid), lying comfortably below Spain's 8.9 G€ hydrogen roadmap budget [7]. The spatial distribution of stations is mapped in Fig. 10.

Optimal renewable installed capacity varies by zone: PV dominates in the South, while hybrid PV–wind ensembles prevail in Central and North Spain, mirroring resource endowments. Fig. 9 illustrates that, despite optimal sizing, off-grid systems, especially PV-heavy southern and Canary sites, still incur substantial curtailment. Grid access alleviates this burden via electricity exports, reducing overall costs.

Electrolyzer full-load hours (FLH) and their implications for greenhouse-gas (GHG) compliance are shown in Fig. 11. FLH are computed as annual grid-supplied electrolyzer energy divided by nominal power. Because a direct RES-electrolyzer link is considered impractical, three attribution scenarios are tested:

- *Conservative:* grid share $=\min(P_{ely}, P_{grid})$ at each timestep.
- *Alternative:* all imported grid energy is assigned to hydrogen production.
- *All-grid:* the entire electrolyzer load is assumed to originate from the grid.

Following Delegated Regulation (EU) 2023/1185 [96], up to H hours (set by the 2023 Spanish market share of RES-marginal pricing, 60.7% or 5317 h [97]) are treated as zero-carbon; excess consumption is penalized at 0.657 kgCO2eq per kWh [98]. All configurations remain below the 3.38 kgCO2eq per kg of hydrogen threshold, even

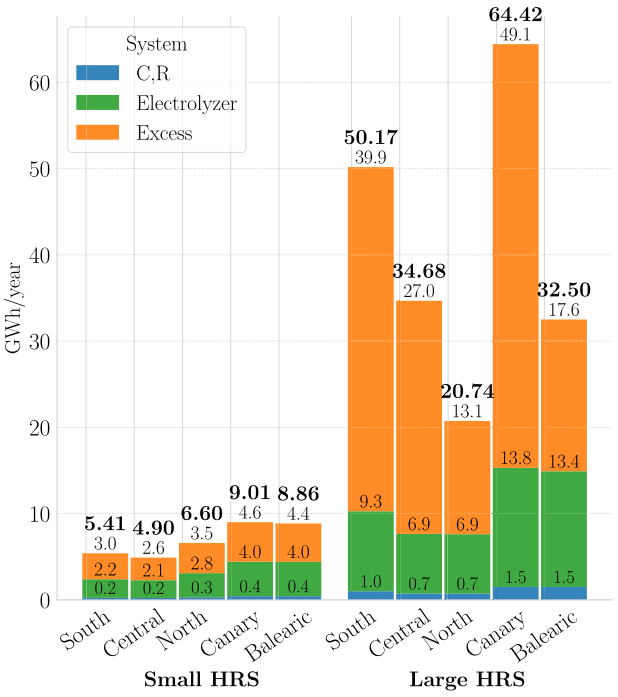

Fig. 9. Energy dispatch breakdown by component, RES-zone and size for off-grid HRSs.

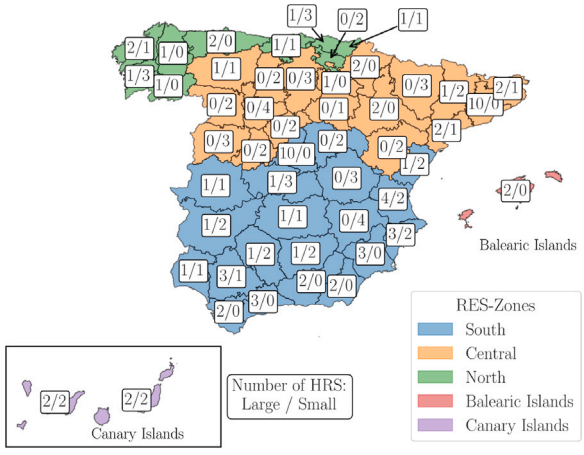

Fig. 10. Optimal allocation of small- and large-sized HRSs per province in Spain by 2030, totalling 149 stations.

under worst-case allocation, since they do not even surpass the 5317 h threshold.

Summarizing, large on-grid HRSs with hybrid PV–wind generation in resource-rich zones offer the most favourable LCOH and NPC, while satisfying EU low-carbon criteria. These results provide actionable guidance for policymakers and investors aiming to scale renewable hydrogen infrastructure across Spain's diverse regions.

Finally, some practical aspects deserve comment. The analysis presented is techno-economic and assumes nominal availability of the main subsystems. In practice, arguably the most limiting factor is the siting of renewable sources relative to the HRS: wind and PV installations require land, clearances and permits that may be impractical in dense urban or insular settings; on-grid cases can also be constrained by interconnection capacity. Thus, the proposed HRS designs are still subject to factors not considered in this study that certainly would affect the results presented. This aspect is discussed Section 5.

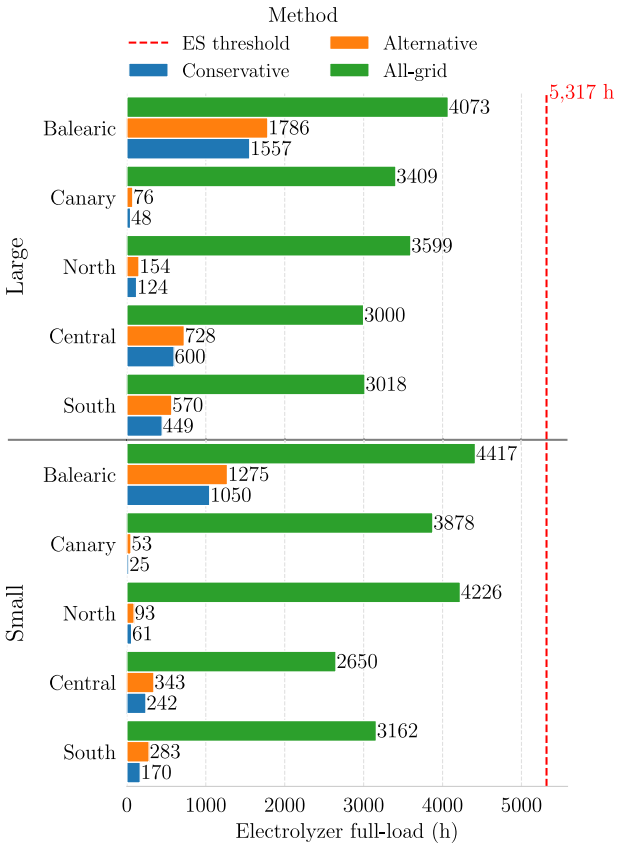

Fig. 11. Electrolyzer full-load hours by RES-zone and attribution scenario for on-grid HRSs, benchmarked against the Spanish threshold of 5317 h.

5. Conclusions

This study aimed to design a green Hydrogen Refuelling Station (HRS) network in Spain to address the significant shortfall in the country's hydrogen infrastructure, which currently comprises only three HRSs and 29 Fuel Cell Electric Vehicles (FCEVs). We employed two tools to achieve this: HDRSAM for detailed HRS modelling and HOMER to evaluate hybrid energy systems incorporating Renewable Energy Sources (RESs). Our projections indicate that in 2030, Spain may present approximately 17,554 light-duty FCEVs and 7700 heavy-duty FCEVs in circulation. In response, the target of the government set between 100 and 150 HRSs was allocated across the Autonomous Communities (AC) based on the existing petrol station distribution to an exact optimal value of 149 stations. A nonlinear programming formulation determined two HRS sizes per geographical cluster and their deployment at a provincial level.

Renewable energy potential was assessed by analysing wind and solar profiles, which led to the division of mainland Spain into five RES-zones: South, Center, North, Canary and Balearic Islands. The economic analysis revealed that off-grid HRSs exhibit Levelized Cost of Hydrogen (LCOH) values ranging from 14.8 $/kg to 24.13 $/kg, with the highest LCOH in Central Spain, and Net Present Costs (NPC) between 13.2 and 18.44 M$ for small stations and 47.86 to 64.42 M$ for large ones. In contrast, grid-connected HRSs achieve lower LCOH values (between 9.56 $/kg and 16.71 $/kg) and NPCs (9.50 to 13.44 M$ for small stations and 24.26 to 43.83 M$ for large stations). The total capital investment for a grid-connected network is estimated at 1.52 G$, well within the planned budget of 8.9 G€.

While this study does not claim to present the definitive solution, it makes a meaningful contribution to the field of hydrogen infrastructure development. Hydrogen technologies offer significant

potential as a clean alternative to carbon-based fuels; however, further research is needed to refine operational strategies, techno-economic models and analysis methodologies. In particular, future work should explore dedicated sensitivity analyses of hydrogen demand explicitly linked to potential Spanish policy measures. It would also be valuable to apply alternative techno-economic models, location methods, or related approaches to the 2030 Spanish context, so that results can be benchmarked against those presented here. At present, there is a general lack of benchmarking or cross-validation in HRS techno-economic studies, since differences in scope, geographical scale, and demand estimation often hinder direct comparison. Addressing this gap would help test, validate and strengthen the methodologies applied in the field. Another relevant extension would be to consider alternative hydrogen production pathways and infrastructure models beyond on-site electrolysis, which may offer different cost and deployment perspectives in future scenarios. Finally, testing the proposed rollout of 149 stations together with their attributed renewable sources against land eligibility, permitting, regional or local policy constraints, social and environmental factors would provide a useful reality check to national roadmaps, which are often optimistic for political reasons. Such an exercise could also yield a practical estimate of the deviation to expect when moving from modelled results to deployable systems, and may even inform simple rule-of-thumb correction factors for studies of a similar scope and methodology to this one. Taken together, these extensions would strengthen the external validity of the present work. The results presented herein, particularly the quantified techno-economic indicators and the optimization-based allocation of 149 HRSs across Spain, stem from a dedicated research effort aimed at assessing the suitability of a hydrogen economy for the future of sustainable mobility in a country with extensive experience and resources in renewable energy infrastructure.

CRediT authorship contribution statement

Beatriz Garcia Minguez: Writing – original draft, Visualization, Validation, Methodology, Investigation, Formal analysis, Data curation, Conceptualization. **Pol Cardona:** Writing – original draft, Visualization, Methodology, Formal analysis, Data curation, Conceptualization. **Luis Valiño:** Writing – review & editing, Validation, Supervision, Resources, Project administration, Methodology, Funding acquisition. **Carlos Ocampo-Martinez:** Writing – review & editing, Validation, Supervision, Project administration, Methodology, Funding acquisition. **Lukas Siemon:** Writing – review & editing, Validation, Supervision, Project administration, Methodology, Investigation, Formal analysis, Conceptualization. **Maria Serra:** Writing – review & editing, Validation, Supervision, Project administration, Methodology, Investigation, Funding acquisition, Formal analysis, Conceptualization.

Declaration of competing interest

The authors declare that they have no known competing financial interests or personal relationships that could have appeared to influence the work reported in this paper.

Acknowledgements

This research has been developed within the CSIC Interdisciplinary Thematic Platform (PTI+) Transición Energética Sostenible+ (PTI-TRANSENER+)[TRE2103000] as part of the CSIC program for the Spanish Recovery, Transformation and Resilience Plan funded by the Recovery and Resilience Facility of the European Union, established by the Regulation (EU) 2020/2094; Project MASHED (TED2021-129927B-I00) funded by MCIN/ AEI /10.13039/501100011033 and by the "European Union NextGenerationEU/PRTR"; and the Project MAFALDA (PID2021-126001OB-C31) funded by MCIN/ AEI /10.13039/501100011033 and by "ERDF A way of making Europe"; Spanish project SEAMLESS: Sustainable learning-based Management of Multi-resource Large-scale Systems (ref. PID2023-148840OB-I00), funded by MCIN/AEI/10.13039/501100011033/FEDER, UE.

Appendix. Additional data

See Tables A.11–A.16.

Table A.11
Vehicle distribution, modal shares, and average refuelling mass by RES zone.

RES Zone	LD-FCEVs	HD-FCEVs	LD Share (%)	HD Share (%)	Avg. Refuel Mass (kg)
South	9550	3953	71	29	7.47
North	2397	896	73	27	7.26
Islands	1383	983	58	42	8.71
Central	4224	1869	69	31	7.61

Table A.12
Provincial ICEV counts, petrol-station shares and initial HRS estimates.

AC	Province	LD-ICEV (vehicles)	HD-ICEV (vehicles)	Petrol Stations	Station share (%)	HRS est.
País Vasco	Álava	174 837	13 586	79	0.67	1
Castilla - La Mancha	Albacete	225 924	27 819	176	1.50	2
Comunitat Valenciana	Alicante/Alacant	1 139 629	95 094	467	3.99	3
Andalucía	Almería	431 682	57 206	224	1.91	2
Castilla y León	Ávila	106 665	12 543	72	0.61	1
Extremadura	Badajoz	437 324	35 973	288	2.46	2
Balears, Illes	Balears, Illes	810 837	87 050	210	1.79	2
Cataluña	Barcelona	2 624 650	208 130	793	6.77	6
Castilla y León	Burgos	217 717	18 573	140	1.20	1
Extremadura	Cáceres	258 679	32 450	164	1.40	2
Andalucía	Cádiz	643 120	52 683	286	2.44	2
Comunitat Valenciana	Castellón/Castelló	353 709	37 735	190	1.62	2
Castilla - La Mancha	Ciudad Real	293 360	36 129	230	1.96	2

(continued on next page)

Table A.12 (*continued*).

AC	Province	LD-ICEV (vehicles)	HD-ICEV (vehicles)	Petrol Stations	Station share (%)	HRS est.
Andalucía	Córdoba	447 151	40 788	262	2.24	2
Galicia	Coruña, A	683 404	47 399	286	2.44	2
Castilla - La Mancha	Cuenca	135 269	19 904	166	1.42	2
Cataluña	Girona	487 736	49 835	259	2.21	2
Andalucía	Granada	547 696	54 603	296	2.53	2
Castilla - La Mancha	Guadalajara	169 018	12 813	96	0.82	1
País Vasco	Guipúzcoa	364 064	29 358	140	1.20	1
Andalucía	Huelva	290 497	30 922	150	1.28	1
Aragón	Huesca	141 808	19 285	132	1.13	1
Andalucía	Jaén	372 113	43 097	258	2.20	2
Castilla y León	León	299 717	27 664	171	1.46	2
Cataluña	Lleida	265 981	34 346	198	1.69	2
Rioja, La	Rioja, La	172 519	19 649	85	0.73	1
Galicia	Lugo	233 604	20 903	131	1.12	1
Madrid, Comunidad de	Madrid	4 439 827	268 401	831	7.10	6
Andalucía	Málaga	986 533	84 562	332	2.83	3
Murcia, Región de	Murcia	885 765	85 992	461	3.94	3
Navarra, Comunidad Foral de	Navarra	381 603	36 288	260	2.22	2
Galicia	Ourense	212 723	20 088	91	0.78	1
Asturias, Principado de	Asturias	574 753	39 387	235	2.01	2
Castilla y León	Palencia	104 995	8189	72	0.61	1
Canarias	Palmas, Las	686 902	118 169	237	2.02	2
Galicia	Pontevedra	597 853	46 347	213	1.82	2
Castilla y León	Salamanca	196 763	18 327	113	0.96	1
Canarias	Santa Cruz de Tenerife	668 135	113 640	228	1.95	2
Cantabria	Cantabria	345 782	29 823	161	1.37	2
Castilla y León	Segovia	104 951	11 698	77	0.66	1
Andalucía	Sevilla	1 038 077	88 373	471	4.02	4
Castilla y León	Soria	59 280	6555	42	0.36	1
Cataluña	Tarragona	478 312	50 238	232	1.98	2
Aragón	Teruel	90 551	12 366	114	0.97	1
Castilla - La Mancha	Toledo	460 594	49 723	317	2.71	3
Comunitat Valenciana	Valencia/Valéncia	1 396 896	128 052	608	5.19	4
Castilla y León	Valladolid	290 296	21 840	165	1.41	2
País Vasco	Vizcaya	565 345	43 753	132	1.13	1
Castilla y León	Zamora	116 302	11 427	90	0.77	1
Aragón	Zaragoza	474 560	39 335	280	2.39	2

Table A.13
Optimized provincial allocation of Small and Large HRSs.

Province	RES Zone	Small HRS (stations)	Large HRS (stations)
Álava	North	2	0
Albacete	South	4	0
Alicante/Alacant	South	2	3
Almería	South	0	2
Ávila	Central	2	0
Badajoz	South	2	1
Balears, Illes	Islands	0	2
Barcelona	Central	0	10
Burgos	Central	3	0
Cáceres	South	1	1
Cádiz	South	0	2
Castellón/Castelló	South	2	1
Ciudad Real	South	1	1
Córdoba	South	2	1
Coruña, A	North	1	2
Cuenca	South	3	0
Girona	Central	1	2
Granada	South	0	2
Guadalajara	South	2	0
Guipúzcoa	North	1	1
Huelva	South	1	1
Huesca	Central	3	0
Jaén	South	2	1
León	Central	1	1
Lleida	Central	2	1
Rioja, La	Central	0	1
Lugo	North	0	1
Madrid	South	0	10
Málaga	South	0	3

(*continued on next page*)

Table A.13 (*continued*).

Province	RES Zone	Small HRS (stations)	Large HRS (stations)
Murcia	South	0	3
Navarra	Central	0	2
Ourense	North	0	1
Asturias	North	0	2
Palencia	Central	2	0
Palmas, Las	Islands	2	2
Pontevedra	North	3	1
Salamanca	Central	3	0
Santa Cruz de Tenerife	Islands	2	2
Cantabria	North	1	1
Segovia	Central	2	0
Sevilla	South	1	3
Soria	Central	1	0
Tarragona	Central	1	2
Teruel	Central	2	0
Toledo	South	3	1
Valencia/Valéncia	South	2	4
Valladolid	Central	4	0
Vizcaya	North	3	1
Zamora	Central	2	0
Zaragoza	Central	0	2

Table A.14
CAPEX and OPEX for HDRSAM cost entries not in HOMER. Codes: SS = South Small, SL = South Large; NS = North Small, NL = North Large; IS = Islands Small, IL = Islands Large; CS = Central Small, CL = Central Large.

Zone–Size	Type	Value	CAPEX (2022 $)	CAPEX (2025 $)	OPEX (2022 $)	OPEX (2025 $)
SS	Refrigeration	12.00	326,955.31	368,478.63	18,358.13	20,689.61
SS	Compressor	11.83	174,478.38	196,637.13	13,286.31	14,973.67
SS	Dispensers	2.00	173,694.75	195,753.98	8,015.80	9,033.80
SS	Electrical	480.00	98,303.57	110,788.12	4,536.59	5,112.73
SS	Control & Safety	0.00	100,000.00	112,700.00	0.00	0.00
SS	Land	396.00	289,046.46	325,755.36	0.00	0.00
SS	Labour	0.00	0.00	0.00	25,601.27	28,852.63
SS	Other	0.00	0.00	0.00	9,735.13	10,971.49
SL	Refrigeration	12.00	326,955.31	368,478.63	17,247.46	19,437.88
SL	Compressor	11.83	174,478.38	196,637.13	12,693.60	14,305.69
SL	Dispensers	2.00	173,694.75	195,753.98	7,425.75	8,368.82
SL	Electrical	480.00	98,303.57	110,788.12	4,202.65	4,736.38
SL	Control & Safety	0.00	100,000.00	112,700.00	0.00	0.00
SL	Land	396.00	340,129.18	383,325.59	0.00	0.00
SL	Labour	0.00	0.00	0.00	36,825.96	41,502.86
SL	Other	0.00	0.00	0.00	11,640.37	13,118.69
NS	Refrigeration	12.00	326,955.31	368,478.63	18,358.13	20,689.61
NS	Compressor	11.83	174,478.38	196,637.13	13,286.31	14,973.67
NS	Dispensers	2.00	173,694.75	195,753.98	8,015.80	9,033.80
NS	Electrical	480.00	98,303.57	110,788.12	4,536.59	5,112.73
NS	Control & Safety	0.00	100,000.00	112,700.00	0.00	0.00
NS	Land	396.00	289,046.46	325,755.36	0.00	0.00
NS	Labour	0.00	0.00	0.00	27,279.10	30,743.54
NS	Other	0.00	0.00	0.00	10,070.69	11,349.67
NL	Refrigeration	12.00	326,955.31	368,478.63	17,247.46	19,437.88
NL	Compressor	11.83	174,478.38	196,637.13	12,693.60	14,305.69
NL	Dispensers	2.00	173,694.75	195,753.98	7,425.75	8,368.82
NL	Electrical	480.00	98,303.57	110,788.12	4,202.65	4,736.38
NL	Control & Safety	0.00	100,000.00	112,700.00	0.00	0.00
NL	Land	396.00	340,129.18	383,325.59	0.00	0.00
NL	Labour	0.00	0.00	0.00	34,165.71	38,504.76
NL	Other	0.00	0.00	0.00	11,108.32	12,519.07
IS	Refrigeration	12.00	326,955.31	368,478.63	18,358.13	20,689.61
IS	Compressor	11.83	174,478.38	196,637.13	13,286.31	14,973.67
IS	Dispensers	2.00	173,694.75	195,753.98	8,015.80	9,033.80
IS	Electrical	480.00	98,303.57	110,788.12	4,536.59	5,112.73
IS	Control & Safety	0.00	100,000.00	112,700.00	0.00	0.00
IS	Land	396.00	289,046.46	325,755.36	0.00	0.00
IS	Labour	0.00	0.00	0.00	29,832.32	33,621.02
IS	Other	0.00	0.00	0.00	10,581.34	11,925.17
IL	Refrigeration	12.00	326,955.31	368,478.63	16,426.84	18,513.04
IL	Compressor	11.83	174,478.38	196,637.13	12,255.68	13,812.15
IL	Dispensers	2.00	173,694.75	195,753.98	6,989.80	7,877.50
IL	Electrical	480.00	98,303.57	110,788.12	3,955.92	4,458.32

(*continued on next page*)

Table A.14 (*continued*).

Zone–Size	Type	Value	CAPEX (2022 $)	CAPEX (2025 $)	OPEX (2022 $)	OPEX (2025 $)
IL	Control & Safety	0.00	100,000.00	112,700.00	0.00	0.00
IL	Land	396.00	391,211.90	440,895.81	0.00	0.00
IL	Labour	0.00	0.00	0.00	40,680.05	45,846.42
IL	Other	0.00	0.00	0.00	12,160.19	13,704.54
CS	Refrigeration	12.00	326,955.31	368,478.63	18,358.13	20,689.61
CS	Compressor	11.83	174,478.38	196,637.13	13,286.31	14,973.67
CS	Dispensers	2.00	173,694.75	195,753.98	8,015.80	9,033.80
CS	Electrical	480.00	98,303.57	110,788.12	4,536.59	5,112.73
CS	Control & Safety	0.00	100,000.00	112,700.00	0.00	0.00
CS	Land	396.00	289,046.46	325,755.36	0.00	0.00
CS	Labour	0.00	0.00	0.00	25,295.83	28,508.40
CS	Other	0.00	0.00	0.00	9,674.04	10,902.64
CL	Refrigeration	12.00	326,955.31	368,478.63	17,247.46	19,437.88
CL	Compressor	11.83	174,478.38	196,637.13	12,693.60	14,305.69
CL	Dispensers	2.00	173,694.75	195,753.98	7,425.75	8,368.82
CL	Electrical	480.00	98,303.57	110,788.12	4,202.65	4,736.38
CL	Control & Safety	0.00	100,000.00	112,700.00	0.00	0.00
CL	Land	396.00	340,129.18	383,325.59	0.00	0.00
CL	Labour	0.00	0.00	0.00	34,207.71	38,552.09
CL	Other	0.00	0.00	0.00	11,116.71	12,528.54

Table A.15
Power converter capacity search space used in HOMER (kW).

Power converter capacities (kW)											
200	300	400	600	800	1000	1400	1800	2200	2600	3000	3400
3800	4200	4600	5000	5500	6000	6500	7000	8000	9000	10 000	

Table A.16
Wind turbine power curve (normalized in terms of the 800 kW ENERCON model) as a function of wind speed.

Wind speed (m/s)	Power (kW)
1	0.0000
2	0.0025
3	0.0175
4	0.0475
5	0.0963
6	0.1763
7	0.2850
8	0.4200
9	0.6000
10	0.8063
11	0.9300
12	0.9750
13	1.0125
14	1.0125
15	1.0125
16	1.0125
17	1.0125
18	1.0125
19	1.0125
20	1.0125
21	1.0125
22	1.0125
23	1.0125
24	1.0125
25	1.0125

References

[1] International Energy Agency. The future of hydrogen: Seizing today's opportunities. Tech. rep., Paris, France: International Energy Agency (IEA); 2019, URL https://www.iea.org/reports/the-future-of-hydrogen.

[2] Ministerio para la Transición Ecológica y el Reto Demográfico. Inventario nacional de emisiones de gases de efecto invernadero: Informe resumen. Edición 1990–2023. Tech. rep., Madrid, España: Dirección General de Calidad y Evaluación Ambiental; 2024, URL https://www.miteco.gob.es/content/dam/miteco/es/calidad-y-evaluacion-ambiental/temas/sistema-espanol-de-inventario-sei-/Documento_resumen_Inventario_GEI.pdf.

[3] Statista. Spain: greenhouse gas emissions share by sector. 2024, https://www.statista.com/statistics/1322798/distribution-of-ghg-emissions-by-sector-spain/. [Accessed 26 August 2024].

[4] Eurostat. Electricity production capacities for renewables and wastes (nrg_inf_epcrw). 2025, URL https://ec.europa.eu/eurostat/databrowser/view/NRG_INF_EPCRW_custom_595641/bookmark/table?lang=en&bookmarkId=da3731be-8c95-436e-801c-ed05c72d4388. [Accessed 4 July 2025].

[5] EurObserv'ER. Photovoltaic Barometer 2023. Tech. rep., EurObserv'ER Consortium; 2023, URL https://www.eurobserv-er.org/photovoltaic-barometer-2023/. [Accessed 4 July 2025].

[6] Genovese M, Fragiacomo P. Hydrogen refueling station: Overview of the technological status and research enhancement. J Energy Storage 2023;61:106758. http://dx.doi.org/10.1016/j.est.2023.106758.

[7] Ministerio para la Transición Ecológica y el Reto Demográfico. Hoja de Ruta del Hidrógeno: Una apuesta por el hidrógeno renovable. Tech. rep., Madrid, España: Gobierno de España; 2020, URL https://www.miteco.gob.es/es/ministerio/planes-estrategias/hidrogeno.html. [Accessed 03 February 2024].

[8] International Energy Agency. Global hydrogen review 2024. Tech. rep., Paris, France: International Energy Agency (IEA); 2024, URL https://www.iea.org/reports/global-hydrogen-review-2024. [Accessed 4 July 2025].

[9] International Energy Agency. Global hydrogen review 2023. Tech. rep., Paris, France: International Energy Agency (IEA); 2023, URL https://www.iea.org/reports/global-hydrogen-review-2023.

[10] Hyundai. ELEC city fuel cell. 2025, https://ecv.hyundai.com/global/en/products/elec-city-fuel-cell-fcev. [Accessed 10 April 2025].

[11] Neugebauer R. Hydrogen technologies. Cham: Springer International Publishing; 2023, http://dx.doi.org/10.1007/978-3-031-22100-2.

[12] Blazquez-Diaz C. Techno-economic modelling and analysis of hydrogen fuelling stations. Int J Hydrog Energy 2019;44(2):495–510. http://dx.doi.org/10.1016/j.ijhydene.2018.11.001.

[13] Micena RP, Llerena-Pizarro OR, de Souza TM, Silveira JL. Solar-powered hydrogen refueling stations: A techno-economic analysis. Int J Hydrog Energy 2020;45(3):2308–18. http://dx.doi.org/10.1016/j.ijhydene.2019.11.092.

[14] Töpler J, Lehmann J. Wasserstoff und Brennstoffzelle. Berlin, Heidelberg: Springer Berlin Heidelberg; 2017, http://dx.doi.org/10.1007/978-3-662-53360-4.

[15] Laboratory AN. Hydrogen refueling station analysis model. 2024, https://hdsam.es.anl.gov/index.php?content=hrsam. [Accessed: 7 June 2024].

[16] European Hydrogen Observatory. Hydrogen fuel cell electric vehicles. 2024, https://observatory.clean-hydrogen.europa.eu/hydrogen-landscape/end-use/hydrogen-fuel-cell-electric-vehicles. [Accessed 4 May 2024].

[17] European Hydrogen Observatory. Hydrogen refuelling stations. 2024, https://observatory.clean-hydrogen.europa.eu/hydrogen-landscape/distribution-and-storage/hydrogen-refuelling-stations. [Accessed 28 April 2024].

[18] S&P Global Commodity Insights. Fuel cell EVs set to top 13 million by 2030 as hydrogen scales up: Hydrogen council. 2020, https://www.spglobal.com/commodityinsights/en/market-insights/latest-news/electric-power/012420-fuel-cell-evs-set-to-top-13-million-by-2030-as-hydrogen-scales-up-hydrogen-council. [Accessed 5 July 2024].

[19] Agency IE. Technology roadmap hydrogen and fuel cells. 2015.

[20] Fuel Cells, Hydrogen 2 Joint Undertaking. Hydrogen roadmap Europe – A sustainable pathway for the European energy transition. Publications Office; 2019, http://dx.doi.org/10.2843/341510.

[21] Iordache M, Schitea D, Iordache I. Hydrogen refuelling station infrastructure roll-up, an indicative assessment of the commercial viability and profitability in the member states of Europe Union. Int J Hydrog Energy 2017;42(50):29629–47. http://dx.doi.org/10.1016/j.ijhydene.2017.09.146.

[22] Fúnez Guerra C, García-Ródenas R, Angulo Sánchez-Herrera E, Rayo DV, Clemente-Jul C. Modeling of the behavior of alternative fuel vehicle buyers. a model for the location of alternative refueling stations. Int J Hydrog Energy 2016;41(42):19312–9. http://dx.doi.org/10.1016/j.ijhydene.2016.07.165.

[23] The Clean Hydrogen Partnership. European hydrogen refuelling stations availability system. 2024, https://h2-map.eu. [Accessed 28 April 2024].

[24] European Alternative Fuels Observatory. Spain. 2024, https://alternative-fuels-observatory.ec.europa.eu/transport-mode/road/spain. [Accessed 5 April 2024].

[25] Transport G-N. Map of iberian natural gas and hydrogen refuelling stations. 2024, https://gasnam.es/mapa-estaciones-gas-natural-hidrogeno/. [Accessed 24 February 2024].

[26] ApS EM. Live map of CO_2 emissions of electricity consumption. 2024, https://app.electricitymaps.com/zone/ES. [Accessed: 28 April 2024].

[27] (UNEF) UEF. Spain is consolidating its position as a major global photovoltaic power, occupying the fourth global ranking of countries with the greatest installed photovoltaic power. 2022, https://www.unef.es/es/comunicacion/comunicacion-post/espana-se-consolida-como-gran-potencia-fotovoltaica-mundial-ocupando-el-cuarto-ranking-global-de-paises-con-mayor-potencia-fotovoltaica-instalada. [Accessed 20 May 2024].

[28] Red Eléctrica - Una empresa de Redeia. Renewables in the spanish electric system. 2023, https://www.sistemaelectrico-ree.es/informe-de-energias-renovables. [Accessed 19 May 2024].

[29] Spanish Wind Energy Association (AEE). Map of wind farms in Spain. 2024, https://aeeolica.org/en/about-wind-energy/map-of-wind-farms-in-spain/. [Accessed 8 May 2024].

[30] Apostolou D, Xydis G. A literature review on hydrogen refuelling stations and infrastructure. current status and future prospects. Renew Sustain Energy Rev 2019;113:109292. http://dx.doi.org/10.1016/j.rser.2019.109292.

[31] Ayodele TR, Mosetlhe TC, Yusuff AA, Ntombela M. Optimal design of wind-powered hydrogen refuelling station for some selected cities of South Africa. Int J Hydrog Energy 2021;46(49):24919–30. http://dx.doi.org/10.1016/j.ijhydene.2021.05.059.

[32] Perna A, Minutillo M, Di Micco S, Jannelli E. Design and costs analysis of hydrogen refuelling stations based on different hydrogen sources and plant configurations. Energies 2022;15(2):541. http://dx.doi.org/10.3390/en15020541.

[33] Linnemann M, Peltzer J. Wasserstoffwirtschaft kompakt. Wiesbaden: Springer Fachmedien Wiesbaden; 2022, http://dx.doi.org/10.1007/978-3-658-39029-7.

[34] Gökçek M, Kale C. Techno-economical evaluation of a hydrogen refuelling station powered by wind-PV hybrid power system: A case study for İzmir-Çeşme. Int J Hydrog Energy 2018;43(23):10615–25. http://dx.doi.org/10.1016/j.ijhydene.2018.01.082.

[35] Gökçek M, Paltrinieri N, Liu Y, Badia E, Dokuz AŞ, Erdoğmuş A, Urhan BB, Yoldaş Ö. Optimum sizing of hybrid renewable power systems for on-site hydrogen refuelling stations: Case studies from Türkiye and Spain. Int J Hydrog Energy 2024;59:715–29. http://dx.doi.org/10.1016/j.ijhydene.2024.02.068.

[36] Rose PK, Neumann F. Hydrogen refueling station networks for heavy-duty vehicles in future power systems. Transp Res Part D: Transp Environ 2020;83:102358. http://dx.doi.org/10.1016/j.trd.2020.102358.

[37] Minutillo M, Perna A, Forcina A, Di Micco S, Jannelli E. Analyzing the levelized cost of hydrogen in refueling stations with on-site hydrogen production via water electrolysis in the Italian scenario. Int J Hydrog Energy 2021;46(26):13667–77. http://dx.doi.org/10.1016/j.ijhydene.2020.11.110.

[38] Šimunović J, Pivac I, Barbir F. Techno-economic assessment of hydrogen refueling station: A case study in Croatia. Int J Hydrog Energy 2022;47(57):24155–68. http://dx.doi.org/10.1016/j.ijhydene.2022.05.278.

[39] Ghaithan AM, Kondkari M, Mohammed A, Attia AM. Optimal design of concentrated solar power-based hydrogen refueling station: Mixed integer linear programming approach. Int J Hydrog Energy 2024;86:703–18. http://dx.doi.org/10.1016/j.ijhydene.2024.08.451, URL https://www.sciencedirect.com/science/article/pii/S0360319924036334.

[40] Maestre VM, Ortiz A, Ortiz I. Decarbonizing the spanish transportation sector by 2050: Design and techno-economic assessment of the hydrogen generation and supply chain. Int J Hydrog Energy 2023;48(99):39514–30. http://dx.doi.org/10.1016/j.ijhydene.2023.05.154.

[41] Barhoumi EM, Okonkwo PC, Farhani S, Ben Belgacem I, Zghaibeh M, Mansir IB, Bacha F. Techno-economic analysis of photovoltaic-hydrogen refueling station case study: A transport company Tunis-Tunisia. Int J Hydrog Energy 2022;47(58):24523–32. http://dx.doi.org/10.1016/j.ijhydene.2021.10.111.

[42] Siyal SH, Mentis D, Howells M. Economic analysis of standalone wind-powered hydrogen refueling stations for road transport at selected sites in Sweden. Int J Hydrog Energy 2015;40(32):9855–65. http://dx.doi.org/10.1016/j.ijhydene.2015.05.021.

[43] Mayyas A, Mann M. Manufacturing competitiveness analysis for hydrogen refueling stations. Int J Hydrog Energy 2019;44(18):9121–42. http://dx.doi.org/10.1016/j.ijhydene.2019.02.135.

[44] Campíñez Romero S, Colmenar-Santos A, Pérez-Molina C, Mur-Pérez F. A hydrogen refuelling stations infrastructure deployment for cities supported on fuel cell taxi roll-out. Energy 2018;148:1018–31. http://dx.doi.org/10.1016/j.energy.2018.02.009.

[45] Chrysochoidis-A. N, Escudé MR, van Wijk AJ. Technical potential of on-site wind powered hydrogen producing refuelling stations in the Netherlands. Int J Hydrog Energy 2020;45(46):25096–108. http://dx.doi.org/10.1016/j.ijhydene.2020.06.125.

[46] Yang C, Hu Q. Quantifying fuel cell vehicles and hydrogen refueling station networks in China based on roadmap. Energy Sustain Dev 2023;76:101265. http://dx.doi.org/10.1016/j.esd.2023.101265.

[47] Yang C, Zeng J-J. Stepwise multi-stage location of hydrogen refueling stations enabled consumer convenience. Int J Hydrog Energy 2025;112:215–21. http://dx.doi.org/10.1016/j.ijhydene.2025.02.371, URL https://www.sciencedirect.com/science/article/pii/S0360319925009553.

[48] Isaac N, Saha AK. A review of the optimization strategies and methods used to locate hydrogen fuel refueling stations. Energies 2023;16(5):2171. http://dx.doi.org/10.3390/en16052171.

[49] Crönert T, Minner S. Location selection for hydrogen fuel stations under emerging provider competition. Transp Res Part C: Emerg Technol 2021;133:103426. http://dx.doi.org/10.1016/j.trc.2021.103426.

[50] Shen W, Li H, Ding H, Zeng M, Xie C, Zhang X. Integrated planning model for optimizing investments in hydrogen infrastructure deployment: A case study of yangtze River Delta Region, China. Energy Sci Eng 2025;13(3):1306–22. http://dx.doi.org/10.1002/ese3.2069, URL https://scijournals.onlinelibrary.wiley.com/doi/abs/10.1002/ese3.2069.

[51] Lin R, Ye Z, Guo Z, Wu B. Hydrogen station location optimization based on multiple data sources. Int J Hydrog Energy 2020;45(17):10270–9. http://dx.doi.org/10.1016/j.ijhydene.2019.10.069.

[52] Homer Energy. Homer® software. 2025, https://www.homerenergy.com. [Accessed 19 February 2025].

[53] Bahramara S, Moghaddam MP, Haghifam MR. Optimal planning of hybrid renewable energy systems using HOMER: A review. Renew Sustain Energy Rev 2016;62:609–20. http://dx.doi.org/10.1016/j.rser.2016.05.039.

[54] Khare V, Nema S, Baredar P. Optimization of hydrogen based hybrid renewable energy system using HOMER, BB-bc and GAMBIT. Int J Hydrog Energy 2016;41(38):16743–51. http://dx.doi.org/10.1016/j.ijhydene.2016.06.228.

[55] Shamsi H, Tran M-K, Akbarpour S, Maroufmashat A, Fowler M. Macro-level optimization of hydrogen infrastructure and supply chain for zero-emission vehicles on a canadian corridor. J Clean Prod 2021;289:125163. http://dx.doi.org/10.1016/j.jclepro.2020.125163.

[56] Kurtz J, Sprik S, Bradley TH. Review of transportation hydrogen infrastructure performance and reliability. Int J Hydrog Energy 2019;44(23):12010–23. http://dx.doi.org/10.1016/j.ijhydene.2019.03.027.

[57] Al-Qahtani A, Parkinson B, Hellgardt K, Shah N, Guillen-Gosalbez G. Uncovering the true cost of hydrogen production routes using life cycle monetisation. Appl Energy 2021;281:115958. http://dx.doi.org/10.1016/j.apenergy.2020.115958.

[58] Halkos GE, Gkampoura E-C. Reviewing usage, potentials, and limitations of renewable energy sources. Energies 2020;13(11):2906. http://dx.doi.org/10.3390/en13112906.

[59] Hau E. Wind turbines. Berlin, Heidelberg: Springer Berlin Heidelberg; 2013, http://dx.doi.org/10.1007/978-3-642-27151-9.

[60] Werth T. Netzberechnung mit Erzeugungsprofilen. Wiesbaden: Springer Fachmedien Wiesbaden; 2016, http://dx.doi.org/10.1007/978-3-658-12728-2.

[61] Enel Green Power. Wind turbine. 2024, https://www.enelgreenpower.com/es/learning-hub/energias-renovables/energia-eolica/aerogenerador.[Accessed 25 May 2024].

[62] Office of Energy Efficiency Renewable Energy – USDepartment of Energy. Wind turbines: the bigger, the better. 2024, https://www.enelgreenpower.com/es/learning-hub/energias-renovables/energia-eolica/aerogenerador. [Accessed 25 May 2024].

[63] Enercon. Wind turbine models E-82 EP2 E4. 2024, https://www.enercon.de/en/turbines/e-82-ep2-e4. [Accessed 26 May 2024].

[64] Frey H, Golze K, Hirscher M, Felderhoff M. Energieträger Wasserstoff. Wiesbaden: Springer Fachmedien Wiesbaden; 2023, http://dx.doi.org/10.1007/978-3-658-40967-8.

[65] Kalogirou SA. Solar energy engineering processes and systems: Chapter 9 - photovoltaic systems. 2023.

[66] Abdulla H, Sleptchenko A, Nayfeh A. Photovoltaic systems operation and maintenance: A review and future directions. Renew Sustain Energy Rev 2024;195:114342. http://dx.doi.org/10.1016/j.rser.2024.114342.

[67] Teh CJQ, Drieberg M, Soeung S, Ahmad R. Simple PV modeling under variable operating conditions. IEEE Access 2021;9:96546–58. http://dx.doi.org/10.1109/ACCESS.2021.3094801.

[68] Kumar S, Lim H. An overview of water electrolysis technologies for green hydrogen production. Energy Rep 2022;8:13793–813. http://dx.doi.org/10.1016/j.egyr.2022.10.127.

[69] Europe H. Clean hydrogen production pathways. 2024, URL https://hydrogeneurope.eu/wp-content/uploads/2024/06/2024_H2E_CleanH2ProductionPathwaysReport.pdf. [Accessed 24 February 2025].
[70] Europe H. Impact assessment of the RED II delegated acts on RFNBO and ghg accounting. 2023, URL https://hydrogeneurope.eu/wp-content/uploads/2023/07/Impact-Assessment-on-the-RED-II-DAs.pdf. [Accessed 24 February 2025].
[71] IRENA. The international renewable energy agency (IRENA) green hydrogen cost reduction: Scaling up electrolysers to meet the 1.5c climate goal. 2020.
[72] Trattner A, Höglinger M, Macherhammer M-G, Sartory M. Renewable hydrogen: Modular concepts from production over storage to the consumer. Chem Ing Tech 2021;93(4):706–16. http://dx.doi.org/10.1002/cite.202000197.
[73] Kumar S, Himabindu V. Hydrogen production by PEM water electrolysis – a review. Mater Sci Energy Technol 2019;2(3):442–54. http://dx.doi.org/10.1016/j.mset.2019.03.002.
[74] Lin Z, Ou S, Elgowainy A, Reddi K, Veenstra M, Verduzco L. A method for determining the optimal delivered hydrogen pressure for fuel cell electric vehicles. Appl Energy 2018;216:183–94. http://dx.doi.org/10.1016/j.apenergy.2018.02.041.
[75] Nistor S, Dave S, Fan Z, Sooriyabandara M. Technical and economic analysis of hydrogen refuelling. Appl Energy 2016;167:211–20. http://dx.doi.org/10.1016/j.apenergy.2015.10.094.
[76] Sdanghi G, Maranzana G, Celzard A, Fierro V. Review of the current technologies and performances of hydrogen compression for stationary and automotive applications. Renew Sustain Energy Rev 2019;102:150–70. http://dx.doi.org/10.1016/j.rser.2018.11.028.
[77] Genovese M, Blekhman D, Dray M, Piraino F, Fragiacomo P. Experimental comparison of hydrogen refueling with directly pressurized vs. Cascade method. Energies 2023;16(15):5749. http://dx.doi.org/10.3390/en16155749.
[78] de Tráfico (DGT) DG. Fleet statistics 2022. 2022, https://www.dgt.es/menusecundario/dgt-en-cifras/dgt-en-cifras-resultados/dgt-en-cifras-detalle/Parque-de-vehiculos-Tablas-estadisticas-2022/. [Accessed 5 May 2024].
[79] bp. Estudio BP sobre hábitos de repostaje en España. 2015, URL https://www.reasonwhy.es/media/library/estudio_de_habitos_de_repostaje_en_espana_2015.pdf. [Accessed 24 February 2025].
[80] Kurtz J, Sprik S, Saur G, Onorato S. Fuel cell electric vehicle driving and fueling behavior. 2018.
[81] Caponi R, Monforti Ferrario A, Del Zotto L, Bocci E. Hydrogen refueling stations and fuel cell buses four year operational analysis under real-world conditions. Int J Hydrog Energy 2023;48(54):20957–70. http://dx.doi.org/10.1016/j.ijhydene.2022.10.093.
[82] Dirección General de Tráfico (DGT). Annualised kilometres travelled by the vehicle fleet 2022. 2022, https://www.dgt.es/menusecundario/dgt-en-cifras/dgt-en-cifras-resultados/dgt-en-cifras-detalle/Kilometros-anualizados-recorridos-por-el-parque-movil-2022/. [Accessed 5 May 2024].
[83] Open Data - Esri. Petrol stations in Spain. 2024, https://opendata.esri.es/datasets/d5c7906b908c48889b45ee823af3f2af/about. [Accessed 28 April 2024].
[84] AMPL Optimization Inc. Amplpy: Python API for AMPL. 2021, https://github.com/ampl/amplpy.
[85] Octeract. Main page. 2025, https://www.octeract.com. [Accessed 22 May 2025].
[86] Boland J, Huang J, Ridley B. Decomposing global solar radiation into its direct and diffuse components. Renew Sustain Energy Rev 2013;(28):749–56. http://dx.doi.org/10.1016/j.rser.2013.08.023.
[87] NASAPrediction Of Worldwide Energy Resources (POWER). Data access viewer (DAV). 2024, https://power.larc.nasa.gov/data-access-viewer/. [Accessed 29 May 2024].
[88] Cardona P, Costa-Castelló R, Roda V, Carroquino J, Valiño L, Ocampo-Martinez C, Serra M. Modelling and operation strategy approaches for on-site Hydrogen Refuelling Stations. Int J Hydrog Energy 2024;52:49–64. http://dx.doi.org/10.1016/j.ijhydene.2023.08.192.
[89] Cardona P, Valiño L, Ocampo-Martinez C, Serra M. Mixed logical dynamical modelling of renewable hydrogen refuelling stations for the design of optimization-based operational schemes. Appl Energy 2025;393:126037. http://dx.doi.org/10.1016/j.apenergy.2025.126037.
[90] International Energy Agency (IEA). Electrolyzers. 2025, https://www.iea.org/energy-system/low-emission-fuels/electrolyzers. [Accessed 29 May 2025].
[91] Trading Economics. Inflation in Spain - march 2025. 2025, https://tradingeconomics.com/spain/inflation-cpi. [Accessed 15 April 2025].
[92] Ẹḍot SIOS - Red Eléctrica de España (REE). Price of excess energy from self-consumption for the simplified compensation mechanism (PVPC). 2024, https://www.esios.ree.es/es/analisis/1739?vis=1&start_date=14-05-2019T00%3A00&end_date=14-05-2019T23%3A00&compare_start_date=13-05-2019T00%3A00&groupby=hour&compare_indicators=1013%2C1014%2C1015. [Accessed 8 July 2024].
[93] OMIE. Electricity prices. 2024, https://www.omie.es/es/spot-hoy. [Accessed 7 August 2024].
[94] Homer Pro. User guide. 2025, https://support.ul-renewables.com/homer-manual-pro/index.html. [Accessed 15 April 2025].
[95] Coppitters D, Verleysen K, de Paepe W, Contino F. How can renewable hydrogen compete with diesel in public transport? Robust design optimization of a hydrogen refueling station under techno-economic and environmental uncertainty. Appl Energy 2022;312:118694. http://dx.doi.org/10.1016/j.apenergy.2022.118694.
[96] European Commission. Commission delegated regulation (EU) 2023/1185 of 10 february 2023 supplementing directive (EU) 2018/2001 of the European parliament and of the council by establishing a minimum threshold for greenhouse gas emissions savings of recycled carbon fuels and by specifying a methodology for assessing greenhouse gas emissions savings from renewable liquid and gaseous transport fuels of non-biological origin and from recycled carbon fuels. 2023, Official Journal of the European Union, L 157, pp. 20–33, URL https://eur-lex.europa.eu/eli/reg/2023/1185/oj. [Accessed 29 May 2025].
[97] Operador del Mercado Ibérico de Energía (OMIE). Informe anual 2023. Annual report, Madrid, Spain: Operador del Mercado Ibérico de Energía — Polo Español, S.A.; 2024, Consulted 29 May 2025. URL https://www.omie.es/sites/default/files/inline-files/Informe_Anual_2023_ES.pdf.
[98] Finance D. Assessing the Impact of Low-Carbon Hydrogen Regulation in the EU. Final report, Deloitte Finance, for Agora Think Tanks gGmbH; 2024, URL https://www.agora-energiewende.org/fileadmin/Partnerpublikationen/2024/2024_Deloitte-Assessing_the_impact_of_low-carbon_hydrogen_regulation_in_the_EU_Final.pdf. [Accessed 29 May 2025].